DECAY OF ^{95}RU AND ^{103}TC

by

Warren Walter Hein

A Dissertation Submitted to the

Graduate Faculty in Partial Fulfillment of

The Requirements for the Degree of

DOCTOR OF PHILOSOPHY

Major Subject: Physics

Approved:

Signature was redacted for privacy.

In Charge of Major Work

Signature was redacted for privacy.

Head of Major Department

Signature was redacted for privacy.

Dean of Graduate College

Iowa State University
Of Science and Technology
Ames, Iowa

1970

TABLE OF CONTENTS

	Page
I. INTRODUCTION	1
A. Historical Review	1
1. Theory	1
2. Experiment	6
a. Decay of ^{95}Ru	6
b. The decay of ^{103}Tc	9
B. Purpose of Investigation	11
II. DECAY OF ^{95}RU	14
A. Source Preparation	14
B. Instrumentation	16
1. Gamma-ray singles measurements	16
2. Gamma-ray coincidence measurements	21
C. Data Analysis	24
D. Results	29
1. Energies and intensities	29
2. Coincidence data	29
3. Decay scheme	33
4. Discussion	43
III. DECAY OF ^{103}TC	45
A. Source Preparation	45
B. Instrumentation	47
1. Gamma-ray singles measurements	47
2. Gamma-ray coincidence measurements	49
C. Data Analysis	54
D. Results	55
1. Energies and intensities	55
2. Coincidence data	61
3. Decay scheme	69
4. Discussion	71

IV. CONCLUSIONS 75

A. Decay of ^{95}Ru 75

B. Decay of ^{103}Tc 77

V. LITERATURE CITED 81

VI. ACKNOWLEDGMENTS 85

I. INTRODUCTION

A. Historical Review

1. Theory

The shell model with spin-orbit coupling was postulated to explain the "magic number" properties of certain nuclei. These nuclei exhibit the same tightly bound structure that was first noticed in the atomic structure of the noble gases. This model has had success in predicting the ground state spins, parities, and nuclear magnetic moments of a large number of nuclei with Z (the number of protons) or N (the number of neutrons) near 2, 8, 20, 28, 50, 82, and 126; the "magic numbers" or shell closures (1, 2).

The mass region with $A \sim 90$ can be treated with an approach based on shell model considerations. As a reminder of what orbitals are being filled for these nuclei, the traditional shell model ordering of proton orbitals taken from Mayer and Jensen (3), is shown in the first figure. For additional reference, a portion of the Chart of the Nuclides (4) showing this mass region is shown in Figure 2.

The first theoretical calculation for this region was not done until 1959, almost ten years after introduction of the shell model. Bayman, Reiner, and Sheline (5) did a detailed spectroscopic calculation using finite-range, spin-dependent central forces of the Yukawa and Gaussian type for ^{90}Zr. Although moderately successful, this approach was difficult to apply to other nuclei in this region.

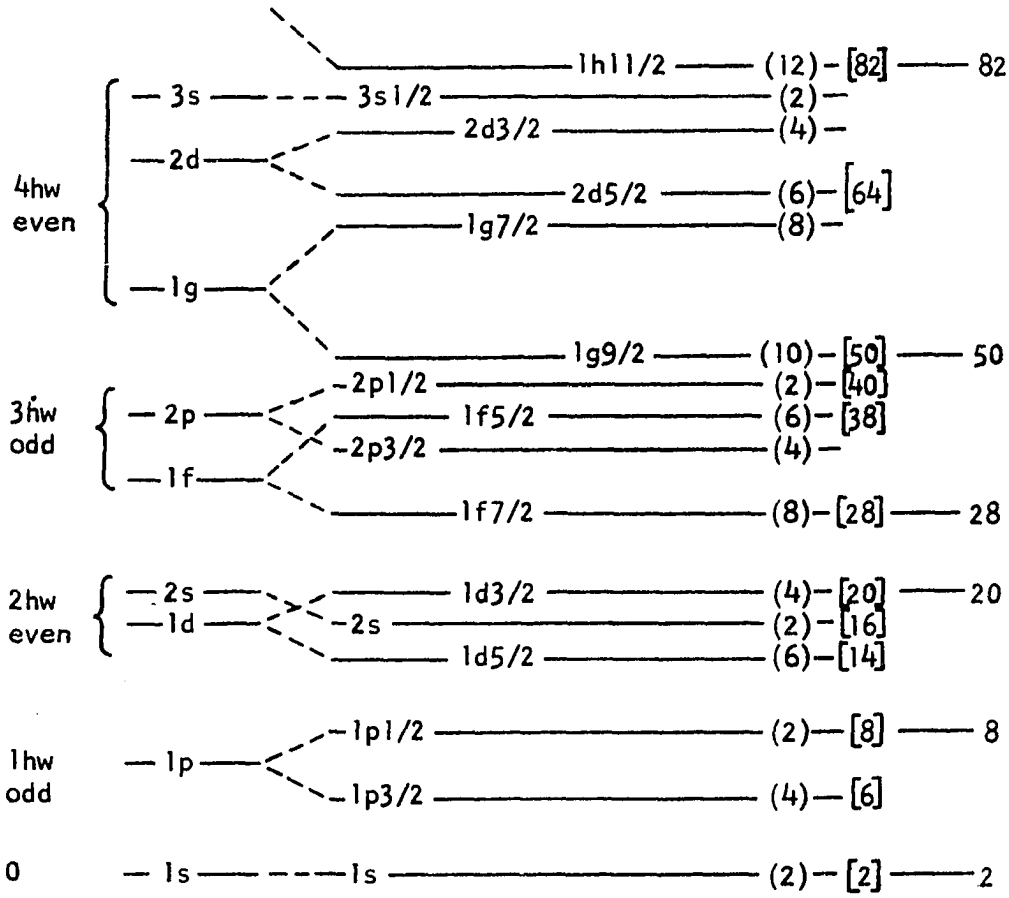

Figure 1. Shell model ordering of protons given in reference (3). The total number of particles and shell closures are shown at the right

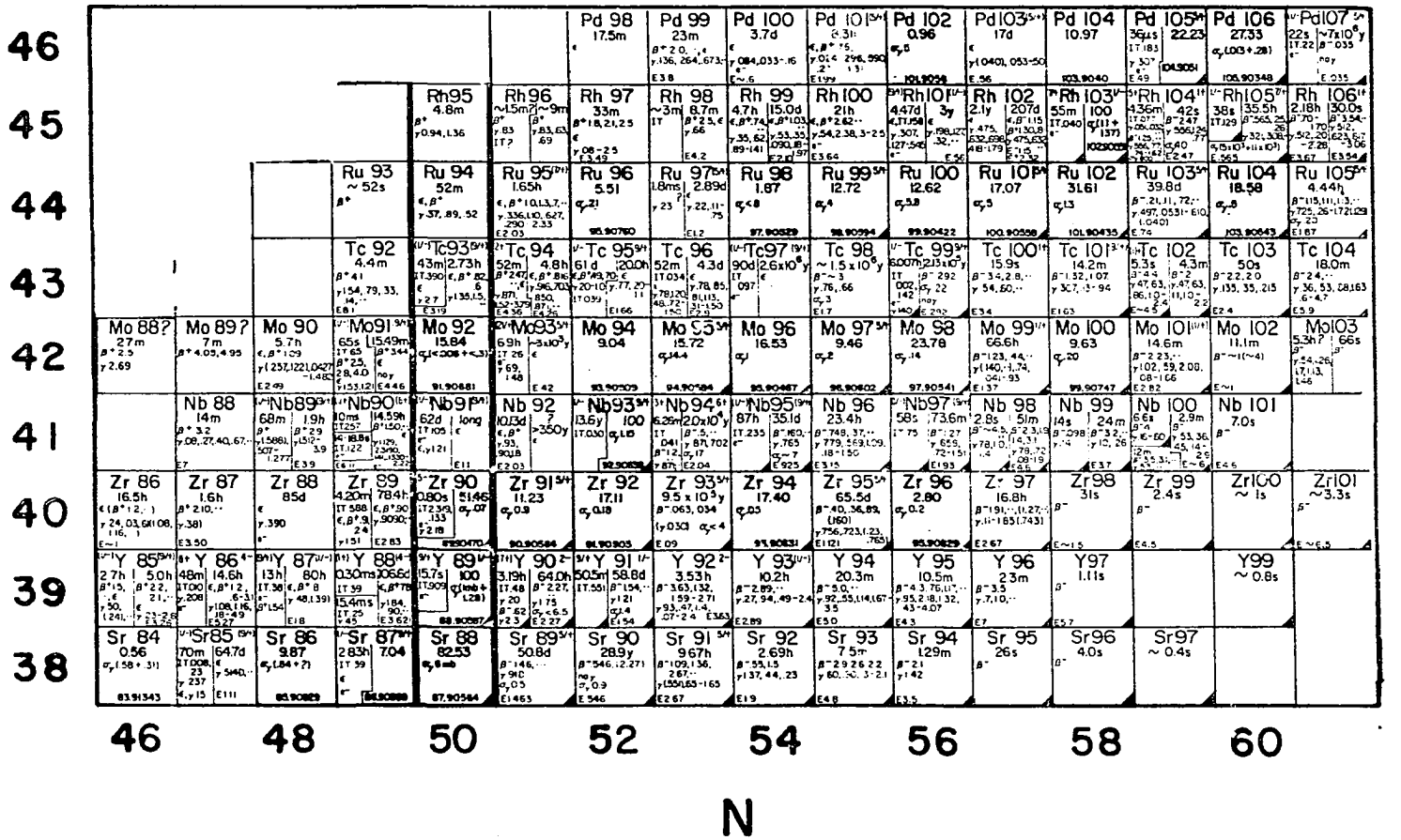

Figure 2. Portion of the Chart of the Nuclides (4) showing the A = 90 mass region

In 1960, Talmi and Unna (6) did a calculation which could be applied to a number of nuclei in this region. Considering $^{88}_{38}Sr$ as an inert core (all proton orbitals filled through $1f_{5/2}$, and all neutrons orbitals filled through $1g_{9/2}$), nuclei were considered with $N = 50$, and $39 \leq Z \leq 43$. The calculation assumed that the potential energy of the nucleus is due to two-body effective interactions between nucleons. The unknown matrix elements of these interactions, considered to be the same for all nuclei in which the same subshells are being filled, were determined from experimental data on other nuclei in this region. Configuration interactions were accounted for in a similar manner. The limited success of this calculation was due mainly to the paucity of experimental data available at this time.

A calculation by Kisslinger and Sorensen (7) in 1963 attempted to describe the $A \sim 90$ isotopes using a quasi-particle-phonon coupling scheme. This treatment showed poor agreement with available experimental data and is not considered to be applicable in this region of the mass table.

More recent calculations by Cohen, Macfarlane, and Soga (8) in 1964, Bhatt and Ball (9) in 1965, Auerbach and Talmi (10) in 1965, and Vervier (11) in 1966 follow the general method of Talmi and Unna (6). All these calculations rely heavily on the use of ^{88}Sr (or ^{90}Zr as in the calculation by Bhatt and Ball) as an inert core. The level schemes for these two nuclei are shown in Figure 3 (12-19). The low density of levels and the large energy gap between the ground state and the first excited state can be used as evidence for partial closure

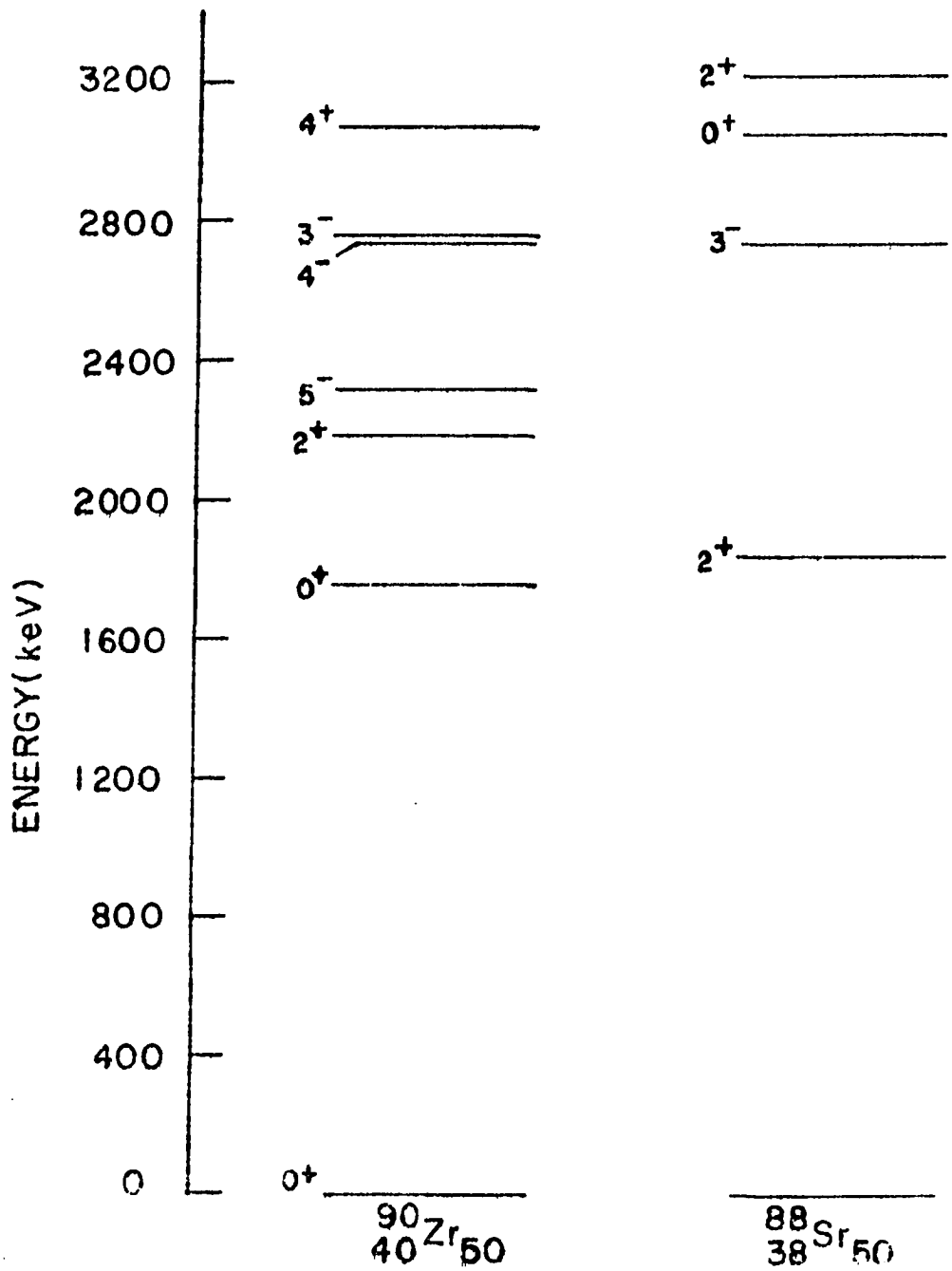

Figure 3. Level structure of ^{90}Zr and ^{88}Sr

at the Z = 38 or Z = 40 subshells. There have been recent direct measurements of this closure using stripping and pickup reactions. Picard and Bassani (20) have found the $1f_{5/2}$ and $2p_{3/2}$ (Figure 1) orbitals to be 90% full in ^{88}Sr. Similarly, Cates (21) has found the $2p_{1/2}$ orbital to be 60% full in ^{90}Zr. In addition, he showed that the proton shell closure for Z = 40 improves as the number of neutrons is increased from N = 50.

From these considerations, it is expected that the ground state of $^{95}_{43}Tc$ will be $9/2^+$, corresponding to the $(1g_{9/2})^5$ and $(2p_{1/2})^2 (1g_{9/2})^3$ configurations of protons. A large number of other positive parity states is also expected, due to the coupling of the protons in the $1g_{9/2}$ orbital to spins ranging from 1/2 to 25/2 (22). In the case of $^{103}_{44}Ru$, the spin and parity of the ground state should be $7/2^+$, corresponding to a $(2d_{5/2})^6(1g_{7/2})^3$ configuration for the neutrons outside the N = 50 closed shell. (Figure 1 is for protons. The ordering for neutrons is similar, but the $2d_{5/2}$ orbital lies below the $1g_{7/2}$.) As for ^{95}Tc, a large number of positive parity levels is expected.

Clearly, the use of ^{88}Sr (or alternatively, ^{90}Zr) as an inert core and the effective interaction approach is by no means an exact solution. However, the relative simplicity of this approach and the success it has had in predicting level sequences seem to justify its use. A comparison between the various theoretical calculations and the experimental work described in this thesis is deferred to Section IV.

2. Experiment

a. Decay of ^{95}Ru Eggen and Pool (23) first produced ^{95}Ru in

1948 and showed it to have a half-life of 1.65 ± 0.05 hours. Since then, the decay of ^{95}Ru to levels in ^{95}Tc has been studied by several investigators (24-26). In addition, levels in ^{95}Tc have recently been investigated by the ^{95}Mo(p,n)^{95}Tc reaction (27). The results of these experiments, which are discussed in the following paragraphs, are summarized in Figure 4.

In 1962, Riehs and Warhanek (24), using NaI(Tl) and anthracene scintillators, observed four gamma rays and a complex positron spectrum in the decay of ^{95}Ru. They placed the highest energy positron group ($E_0 \approx 1.33$ MeV) as an allowed transition to the ground state, deducing $Q_{EC} \approx 2.35$ MeV. Assuming a ground state spin and parity of $9/2^+$ for ^{95}Tc, they assigned a ground state spin and parity of $7/2^+$ to ^{95}Ru. This does not agree with the shell model prediction of $5/2^+$, corresponding to the 51st neutron occupying a $1d_{5/2}$ orbital.

The value $Q_{EC} \approx 2.35$ is inconsistent with the later observation by Heuer (25) of a moderately intense 2.33 MeV gamma ray. The K-shell binding energy is 22 keV (28) for ruthenium and this makes the log (ft) for feeding of the 2.33 MeV level in ^{95}Tc unphysically small. Using Ge(Li) and Si(Li) detectors, Heuer measured energies and intensities of 14 other gamma rays and determined the total conversion coefficient for the intense 336 keV transition to be $9.6 \pm 2 \times 10^{-3}$, from which he deduced M1 multipolarity (29). On the basis of this multipolarity, he assigned a possible spin and parity of $7/2^+$ to the 336 keV level. However, he did not measure the positron spectrum and the inconsistency between his data, the shell model prediction, and the

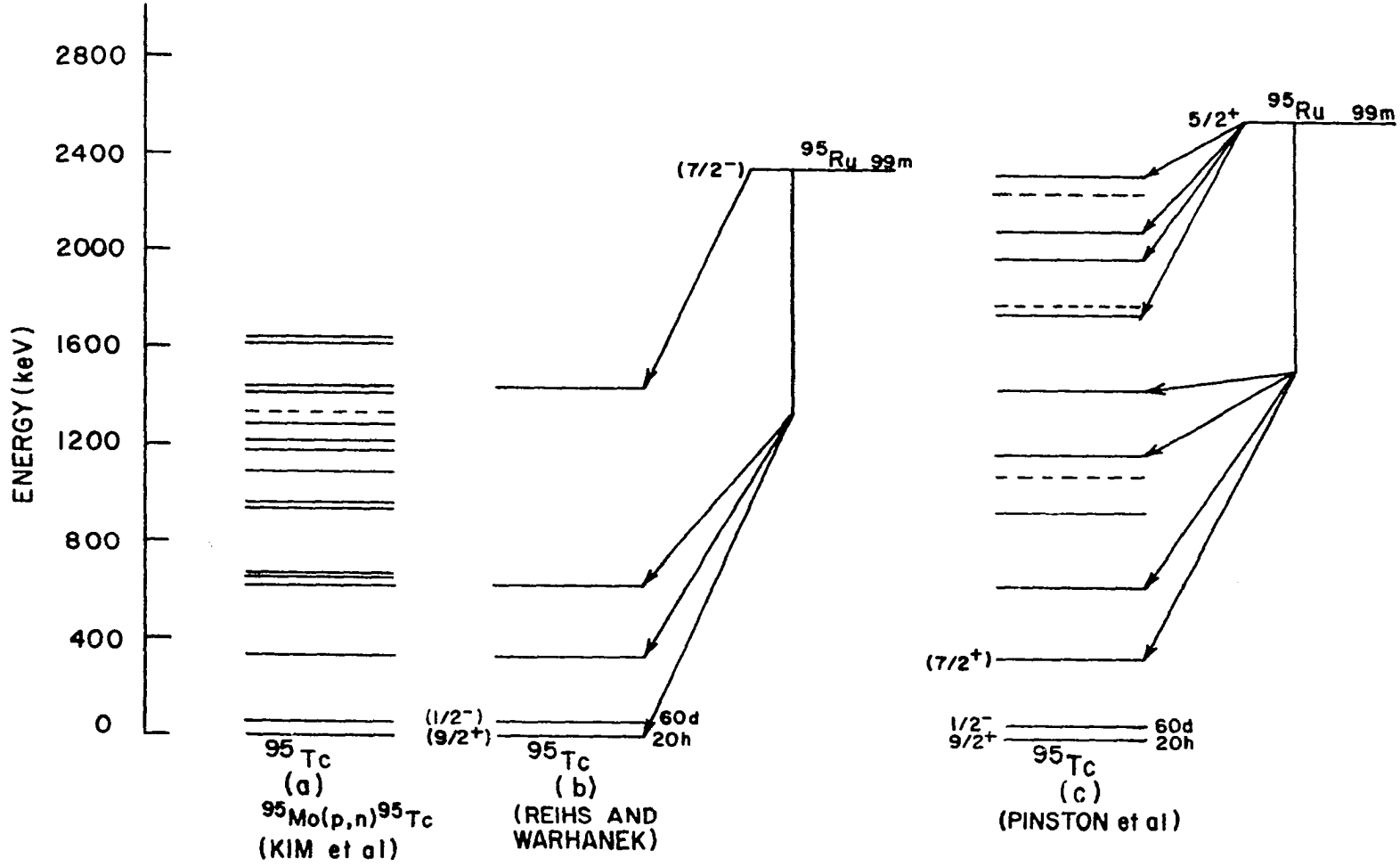

Figure 4. Previous studies of the decay of ^{95}Ru and the energy levels of ^{95}Tc

data of Riehs and Warhanek remained.

This inconsistency was resolved by the beta-gamma coincidence studies of Pinston, Monnand, and Moussa (26). They reported the maximum energy beta group as feeding an excited state at 336 keV instead of the ground state. This makes an assignment of $5/2^+$ possible for the ground state of ^{95}Ru and also increases Q_{EC} to $\approx$ 2.69 MeV, in agreement with shell model predictions and the experiment of Heuer. These results have been confirmed recently by Ball (30) in his ^{96}Ru(p, d) work.

In addition to their beta decay work, Pinston et al. assigned twenty-one gamma rays to the decay of ^{95}Ru on the basis of Ge(Li) singles spectra and Ge(Li)-NaI(Tl) coincidence data.

Recently, Kim et al, (27) have studied the levels of ^{95}Tc through the ^{95}Mo(p, n) reaction. If only s-, p-, and d-wave protons contribute to compound nucleus formation, residual states in ^{95}Tc with spins ranging from 1/2 to 15/2 could be populated. Since the selection rules for reactions differ from those of beta decay, the sequence of final states is not the same.

b. The decay of ^{103}Tc Very little experimental data exists for the decay of ^{103}Tc to excited states of ^{103}Ru. In 1963, Kienle, Wien, Zahn, and Weckermann (31) obtained ^{103}Tc by a second sublimation from the fission products of uranium. The decay of ^{103}Tc was investigated using scintillation counters and coincidence methods. They found two beta groups at energies of 2.0 MeV and 2.2 MeV followed by gamma rays of 350, 215, and 135 keV. From their data, they proposed

a Q-value of 2.35 ± 0.10 MeV corresponding to levels at 135 and 350 keV, with no allowed beta feeding of the ^{103}Ru ground state.

In 1964, Brandi, Engelmann, Hepp, Kluge, Krehbiel, and Meyer-Berkhaut (32) used the ^{104}Ru(γ,n) reaction to find a short-lived isomeric state in ^{103}Ru. A 212 keV gamma ray was observed to decay with half-life 1.7 ± 0.3 milliseconds. This energy agrees with one of the gamma rays reported by Kienle et al., but the coincident 135 keV transition observed in the earlier work to follow the 215 keV gamma was not seen. A similar experiment by Gabsdil (33) in 1968 showed this gamma ray to have an energy of 209 ± 0.5 keV, and again no 135 keV gamma ray was seen in coincidence with it ($I_{135} \leq 0.1\ I_{209}$).

Besides these decay studies, Diehl, Cohen, and Moyer (34) have studied the levels of ^{103}Ru through the reaction ^{104}Ru(d,t)^{103}Ru and have assigned a ground state spin and parity of $5/2^+$ to ^{103}Ru. They reported another fifteen levels for which they assigned spins and parities.

A second reaction experiment which gives information about the levels of ^{103}Ru is the ^{102}Ru(d,p)^{103}Ru work of Nolen, Fortune, Kienle, and Morrison (35). The levels seen in this work were also seen in the (d,t) work of Diehl et al., and the spin and parity assignments are the same in most cases. However, a number of levels were seen in the (d,t) work that were not seen in the (d,p) experiment. In general, different selection rules apply to these two experiments. The (d,p) work excites the particle states, while the (d,t) work tests the hole states. The reaction experiments, as well as the beta decay

work of Kienle et al., are summarized in Figure 5.

B. Purpose of Investigation

An accurate determination of the level structure of a nucleus requires that the nucleus be studied by both reaction processes and spontaneous decay of neighboring nuclides. Until recently, very little reaction work was available to compare with theory or decay data. The new reaction data has made it necessary to restudy many nuclides by the decay mechanism.

The nuclides in the A $\sim$ 90 region are of particular interest. The present work on ^{95}Ru investigates some specific questions which arose from the work of Pinston et al. (26). First, there were a number of weak gamma rays in the singles spectrum which could not be placed in the decay scheme. The use of beta branching ratios and gamma-ray branching to determine spins and parities requires the placement of as many transitions as possible. In addition, the spectrum observed by Pinston et al. was too complex to be resolved by their Ge(Li)-NaI(Tl) coincidence experiment. Ge(Li)-Ge(Li) coincidence data should be a significant improvement.

Another isotope of interest in this mass region is ^{93}Ru. ^{93}Ru decays by electron capture and positron emission to levels in ^{93}Tc, a 50 neutron nucleus, with a reported half-life of 50 seconds (4, 28). Gamma rays which decayed with this half-life were seen in an experiment with natural ruthenium. However, using a sample enriched to 98% in ^{96}Ru, no gamma rays with a 50 second half-life were seen. This implies

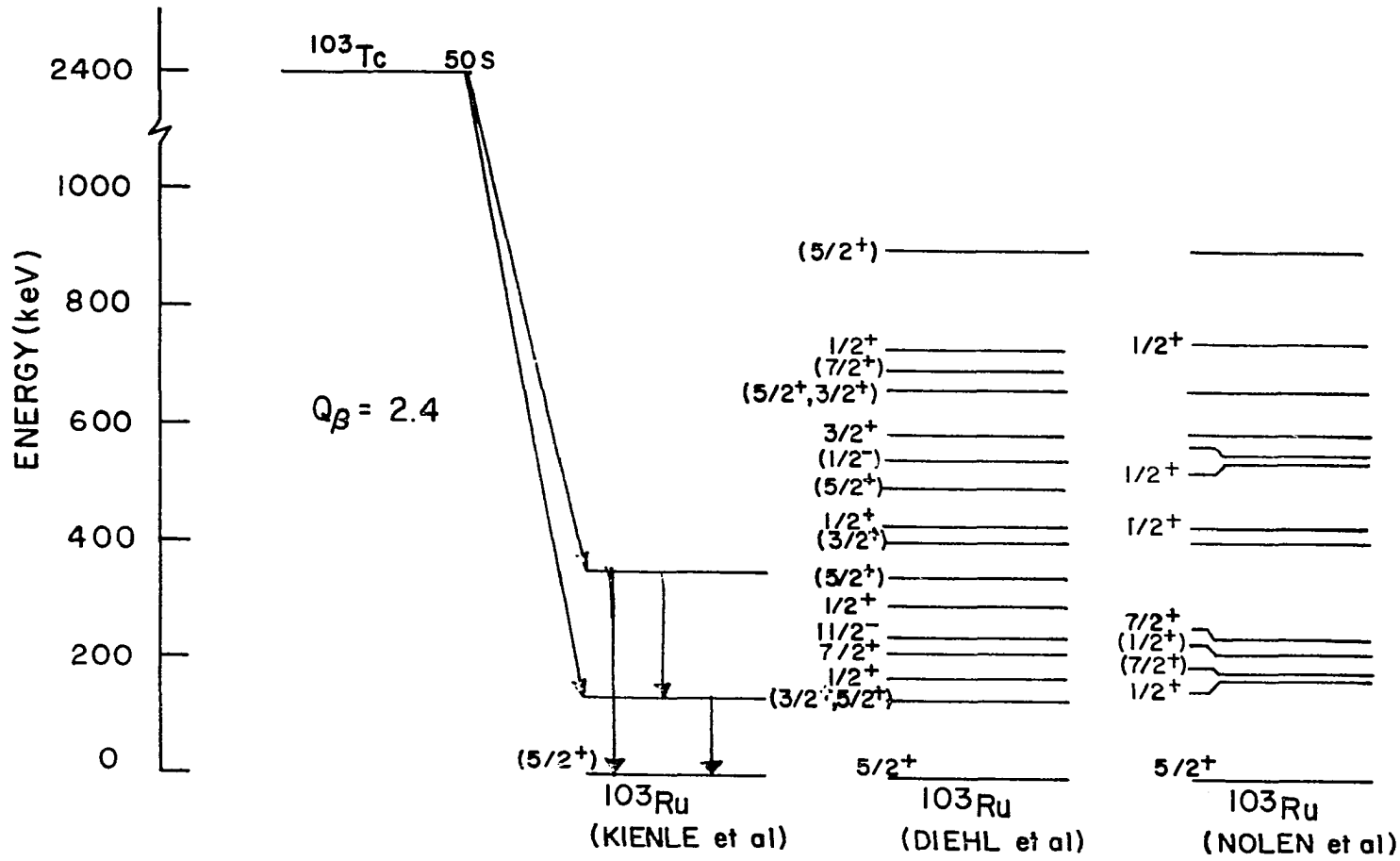

Figure 5. Previous study of the decay of ^{103}Tc and the energy levels of ^{103}Ru

that ^{93}Ru must decay almost entirely to the ground state of ^{93}Tc.

The 50 second activity seen in the irradiation of natural ruthenium was due to the decay of ^{103}Tc. The small number of levels and transitions seen by Kienle et al. (31) compared to the number of levels reported in the reaction work of Diehl et al. (34) makes a restudy of the ^{103}Tc decay an interesting project. The availability of high resolution and high efficiency Ge(Li) detectors should be a significant improvement over the NaI(Tl) work of Kienle et al. Since ^{103}Ru has 6 protons and 9 neutrons outside the ^{88}Sr core, the level structure can not be expected to be described accurately by the calculations discussed in Section I., A.

II. DECAY OF ^{95}RU

Information on the properties of levels in ^{95}Tc can be obtained by studying the positron decay of 99 minute ^{95}Ru. The ground state of ^{95}Tc has been assigned a spin and parity of $9/2^+$ in agreement with the shell model prediction (Figure 1) (26). In addition, a $1/2^-$ isomeric state has been identified at 38.9 keV (36) and $7/2^+$ level at 337 keV (25) (Figure 4). However, no other spin and parity assignments have been made. This makes a detailed comparison with various theoretical treatments (6, 8-11) difficult. This chapter discusses the use of a Ge(Li) detector in a Compton suppression system and Ge(Li)-Ge(Li) coincidence spectrometers to obtain new information about the decay of ^{95}Ru to ^{95}Tc.

A. Source Preparation

Sources of radioactive ^{95}Ru were produced by the ^{96}Ru(γ,n)^{95}Ru reaction using the 70 MeV Electron Synchrotron at Iowa State University. The method used to produce intense sources is illustrated in Figure 6. The electron beam is directed into the target material, producing intense bremsstrahlung as it is stopped. The spread of the beam perpendicular to the plane of the drawing is roughly one millimeter. A detailed description has been published previously (37-39).

A 2.4 gram natural ruthenium metal target was used in these experiments. Natural ruthenium is 5.51% ^{96}Ru with 1.87% ^{98}Ru, 12.72% ^{99}Ru, 12.62% ^{100}Ru, 17.07% ^{101}Ru, 31.61% ^{102}Ru, and 18.58% ^{104}Ru. These isotopes give rise to a number of activities when the natural ruthenium

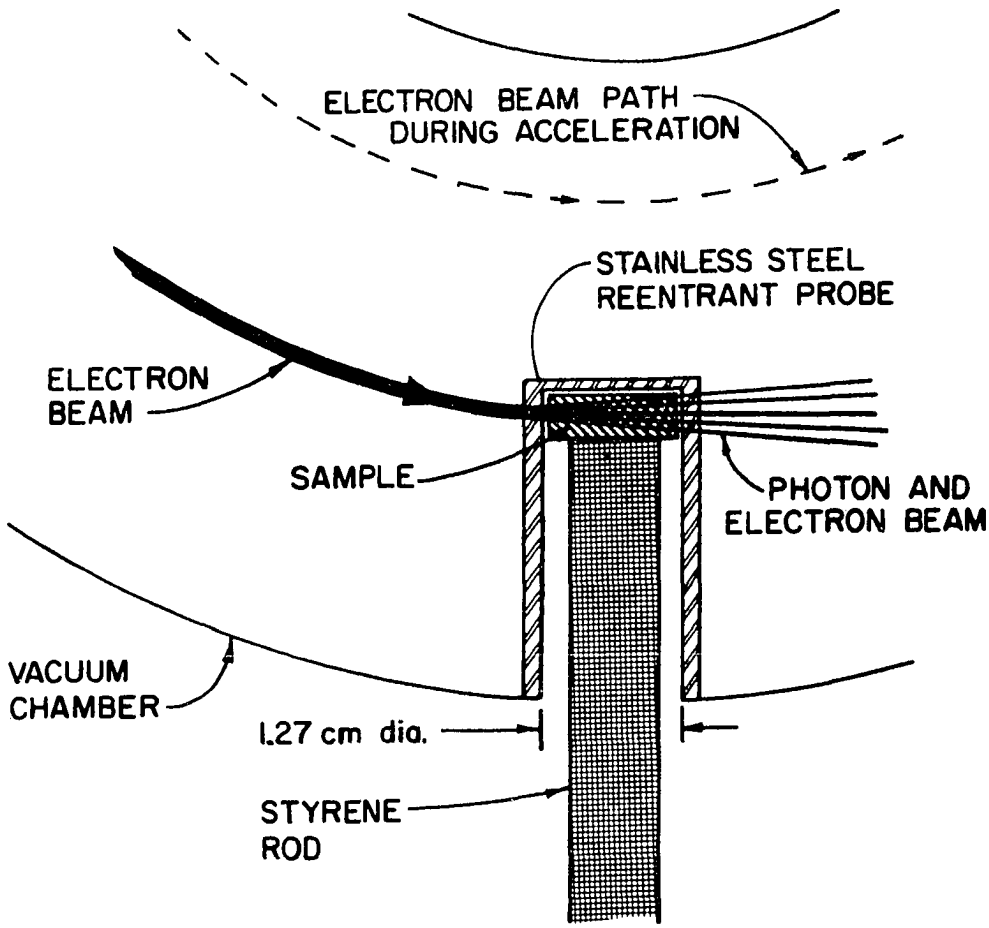

Figure 6. The Synchrotron irradiation geometry

target is irradiated. Among these background activities are the 2.7 hour ^{93}Tc, 52 minute and 4.8 hour ^{94g,m}Tc, 53 minute ^{94}Ru, 20 hour ^{95}Tc, 14 minute ^{101}Tc, 40 day ^{103}Ru, 4 minute ^{102}Tc, and 50 second ^{103}Tc. However, none of these have a half-life close to the 99 minute half-life of ^{95}Ru and are easily distinguished from it. The metal target was bombarded for 30 minutes and allowed to cool 16 minutes while the sample was being transported from the synchrotron to a counting laboratory in the physics building. This procedure reduced the amount of short-lived activity present in the sample.

B. Instrumentation

1. Gamma-ray singles measurements

A 23 cc Ge(Li) detector was used for energy and intensity measurements. This detector had a resolution better than 3.5 keV FWHM and a peak-to-Compton of 9-1 at 1.332 MeV. To enhance weak peaks in the gamma-ray spectrum, the Ge(Li) detector was partially surrounded by a NaI(Tl) scintillator operated in anticoincidence. The scintillator consisted of two 12.7 centimeter diameter by 7.6 centimeter long cylinders with hemicylindrical slots machined in the front faces to match the end cap of the Ge(Li) detector cryostat as shown in Figure 7. This detector was operated in a Compton suppression mode of the type previously described by Orphan and Rasmussen (40) and Simmons (41). The gamma rays were collimated by a 1.8 centimeter aperture in a 5.1 centimeter thick lead shield. Coincident signals in the Ge(Li) detector and either NaI(Tl) scintillator were interpreted as Compton scattering

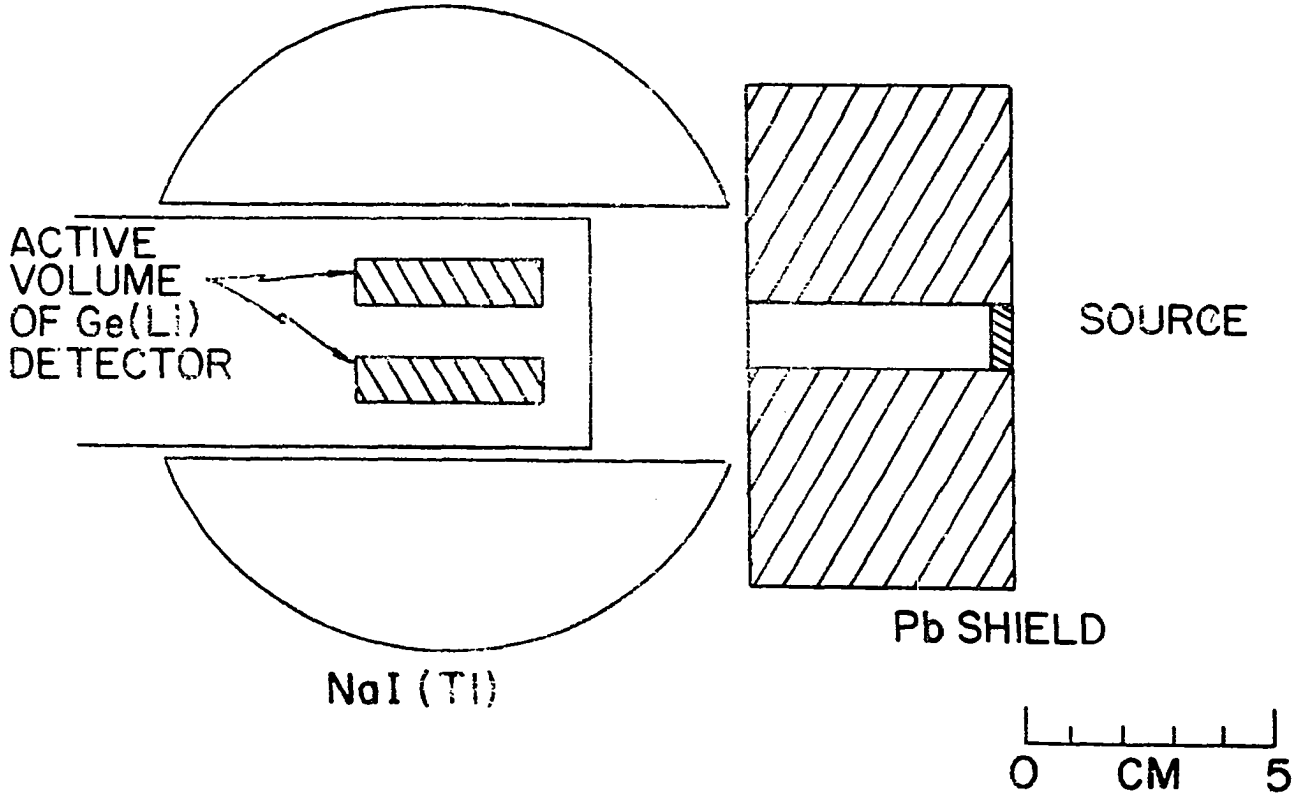

Figure 7. Cross section of detector configuration for Compton suppression system

events, and the corresponding pulse from the Ge(Li) detector was not recorded. If a gamma ray deposited all of its energy in the Ge(Li) detector, the pulse was amplified and recorded in a 4096-channel pulse height analyzer. In this way the peak-to-Compton ratio could be improved by a factor of 2 or 3.

A block diagram of the electronics for this detector arrangement is shown in Figure 8. Double delay line pulse shaping and cross-over timing were used in the two NaI(Tl) channels, with both of the timing single channel analyzers operated in the discriminator mode. Leading edge timing was used in the Ge(Li) channel. Pulses from the preamp were amplified by a commercial "active filter" amplifier for which time constants and pole/zero cancellation were adjusted to maximize the energy resolution.

The relative detection efficiency of this system as a function of gamma-ray energy is shown in Figure 9. The relative efficiency of the detector system for a peak in the calibration spectrum is given by:

$$\text{relative efficiency} = \frac{\text{relative area in spectrum}}{\text{known relative intensity}} .$$

The relative area is the peak area divided by the area of the most intense peak in the spectrum, and the relative intensity is the known gamma-ray branching for the peak of interest divided by the known branching of the most intense peak. This was measured using ^{226}Ra as a source, for which accurate energies and intensities are known (42).

The gain and zero settings of the amplifier-analyzer system were

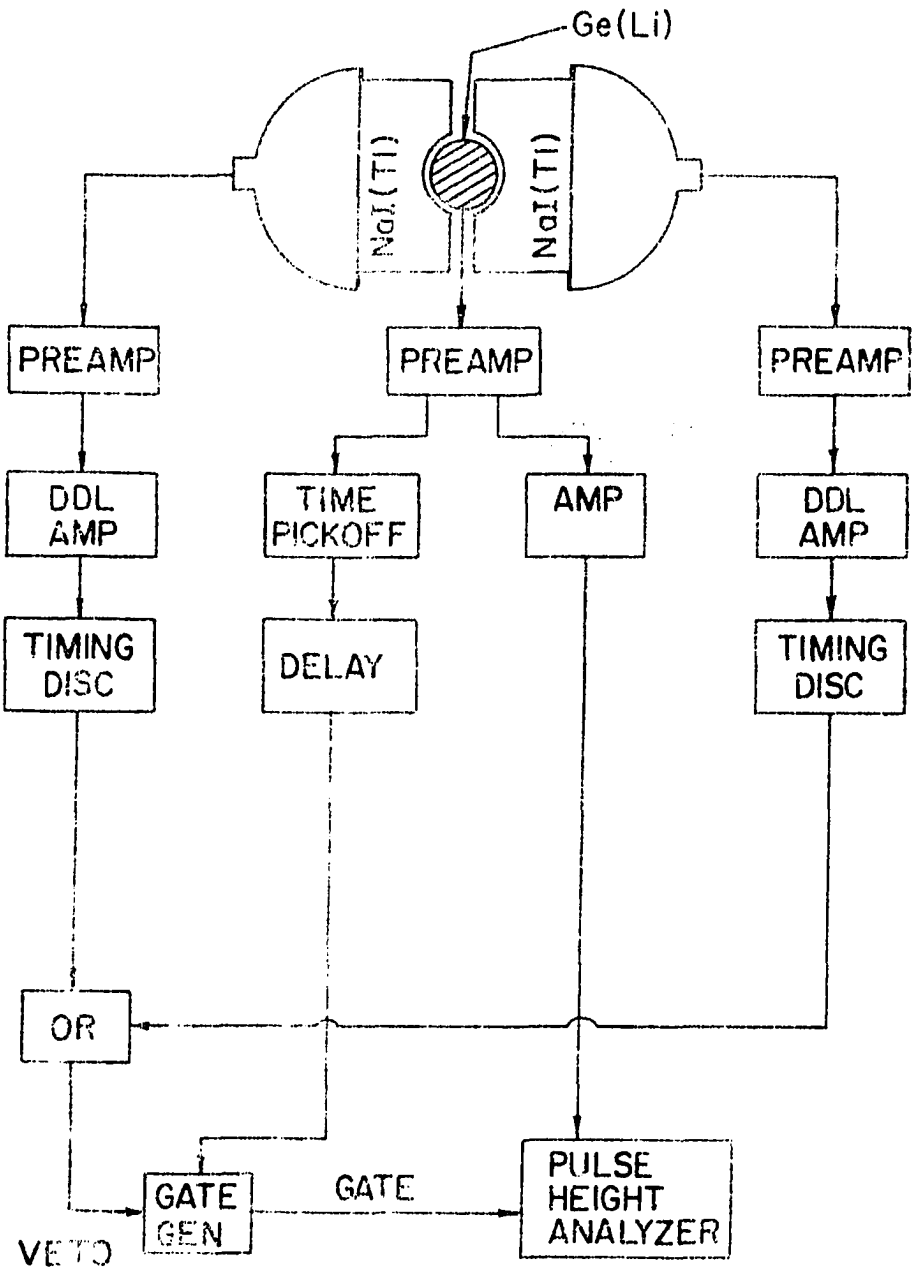

Figure 8. Electronics for Compton suppression system

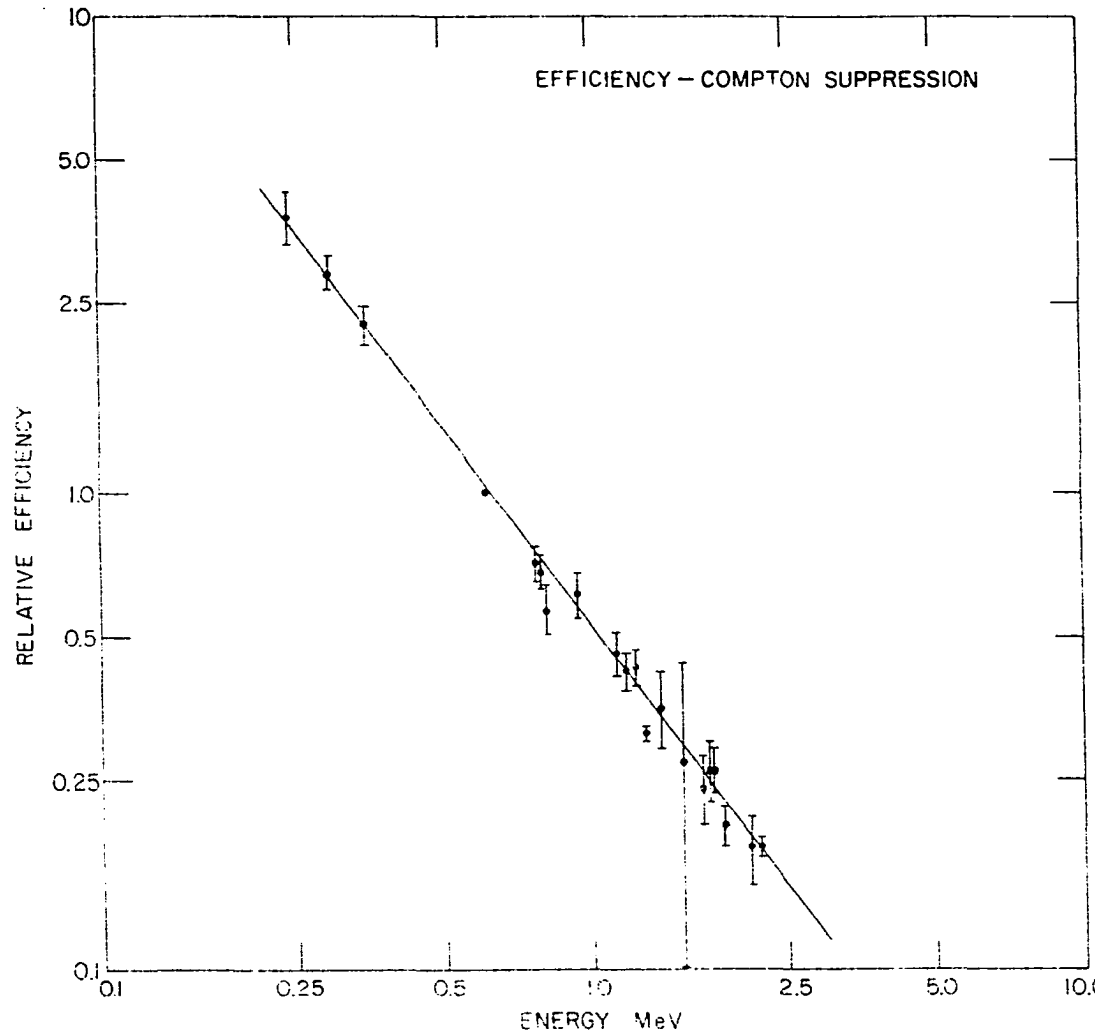

Figure 9. Relative efficiency of Compton suppression system

adjusted so gamma rays with energies between 100 and 2400 keV could be studied. A typical spectrum taken with this detector system is shown in Figure 10. Gamma rays which belong to the decay of ^{95}Ru are labelled by their energy to the nearest keV. Prominent gamma rays which belong to other activities produced in the bombardment of natural ruthenium are labelled by both their energy and origin. The assignment of gamma rays is discussed in Section II., C. Sample decay curves are also shown there.

2. Gamma-ray coincidence measurements

The decay of ^{95}Ru is too complex to be adequately resolved by the Ge(Li)-NaI(Tl) coincidence measurements reported by Pinston et al. (26). The recent development of large Ge(Li) detectors has made Ge(Li)-Ge(Li) coincidence measurements feasible. In this experiment, pulses in a 65 cc Ge(Li) detector (3.5 keV FWHM resolution at 1.332 MeV) was used to gate the signals in a 25 cc Ge(Li) detector (3.4 keV FWHM resolution at 1.332 MeV). These detectors were positioned at 90 degrees relative to one another to minimize the number of 511-511 keV coincidences. The block diagram for this detector arrangement is shown in Figure 11. The preamp signal from both detectors was split and sent through linear amplifiers for energy analysis, and through double delay line amplifiers for timing purposes. Cross-over timing was used in both channels with a resulting resolving time of 75 nanoseconds. In the gating channel, a broad window (approximately 50 keV) was set by the timing single channel analyzer on the spectral region of interest. Narrow windows (approximately 5 keV wide) were then set with the single

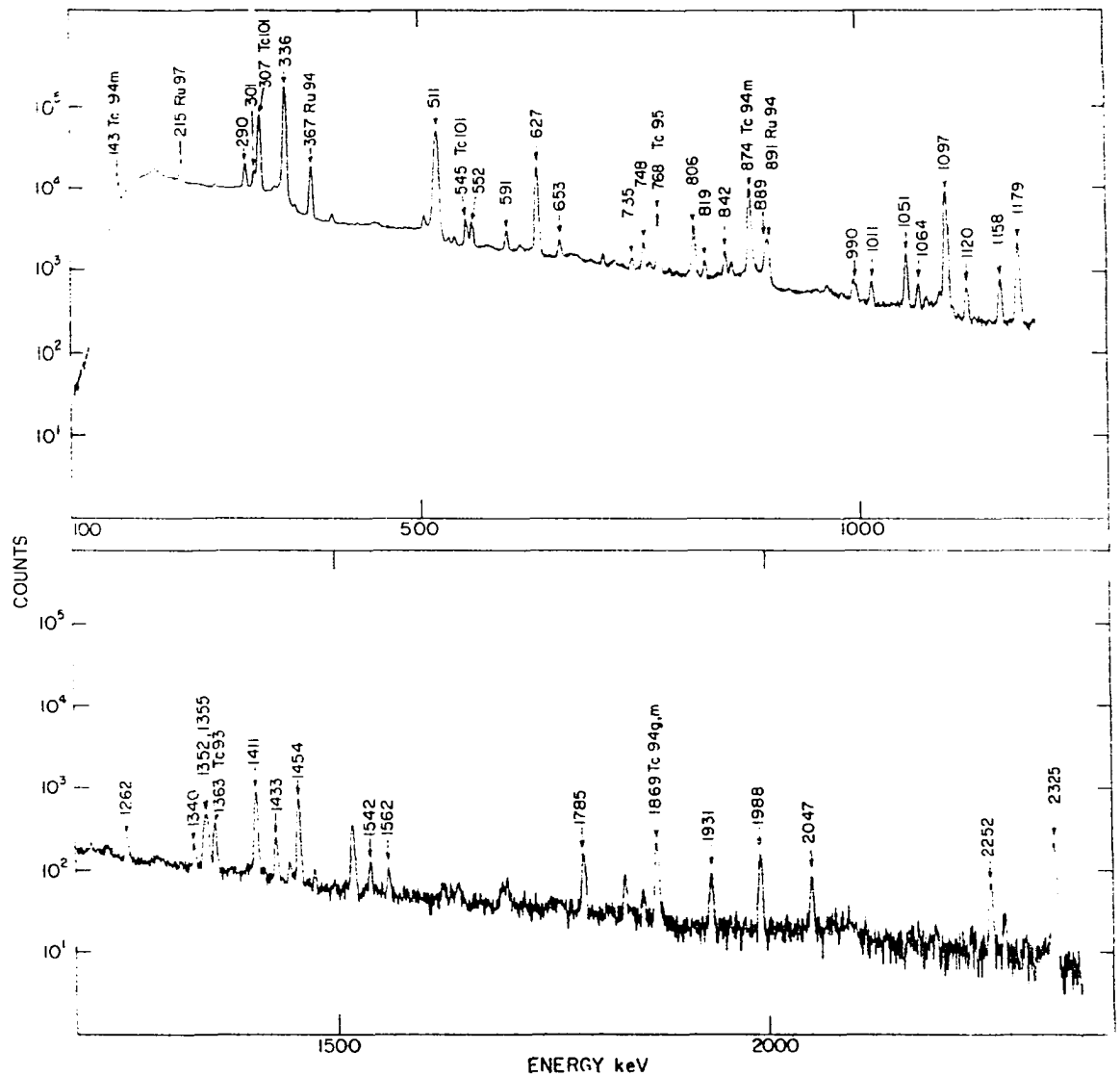

Figure 10. Spectrum of ^{95}Ru gamma rays observed with Compton suppression system

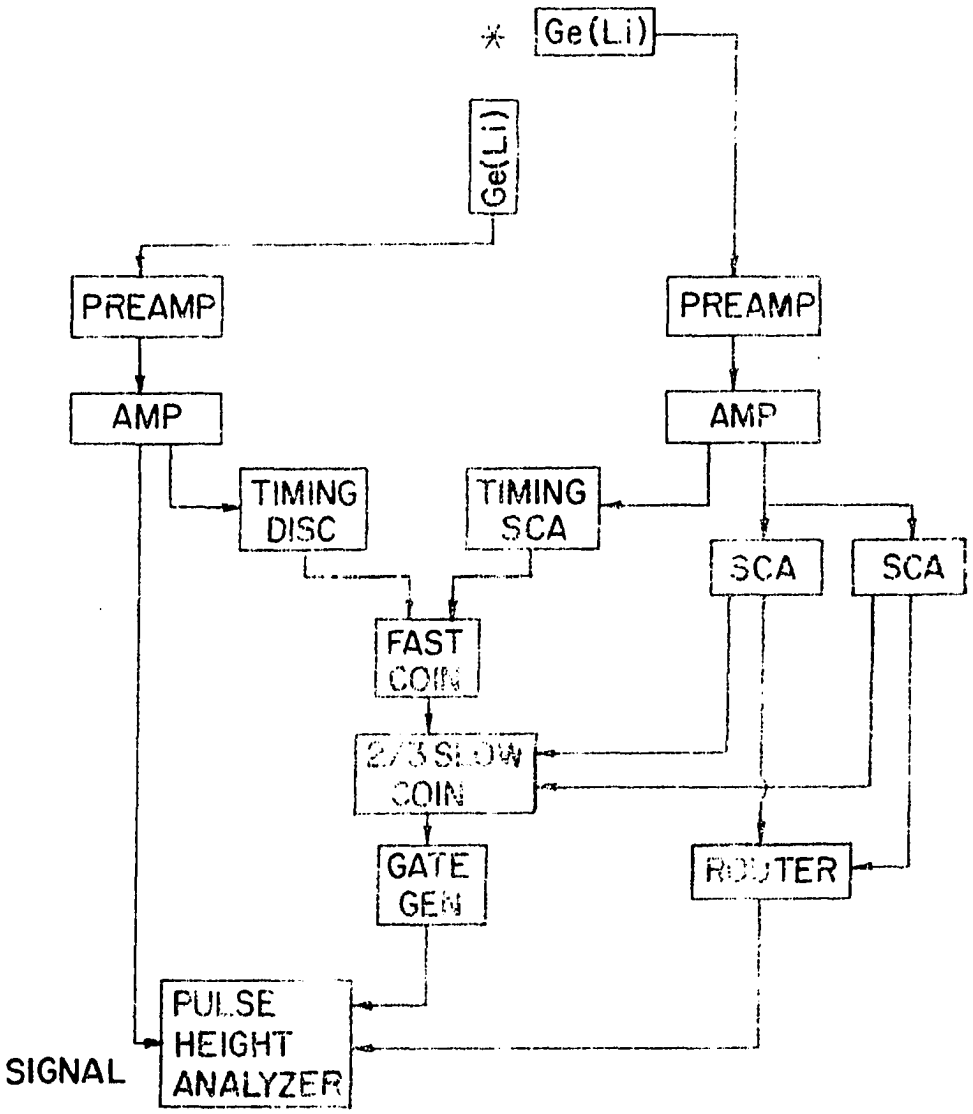

Figure 11. Electronics for coincidence experiment

channel analyzers on the spectral peak to be used as the gating signal and on a flat portion of the background near this peak. Pulses in the other Ge(Li) detector coincident with either of these signals were routed into separate halves of the multichannel analyzer memory.

This detector system was used to record coincidences with the 336, 627, 1051, and 1096 keV gamma rays from the decay of ^{95}Ru. In each case, the sample was irradiated for 30 minutes and then counted for several hours.

C. Data Analysis

The irradiated ruthenium sample was studied with the Compton suppression system described earlier. A sequence of seven 40 minute counts was taken over a period of 6 hours to follow the 99 minute ^{95}Ru activity. Peak positions and areas were calculated by the computer codes PEAKFIND and SKLN available at this laboratory.[1] The first of these is a peak search and fitting program which finds peaks and then fits a Gaussian function with a low-energy exponential tail and a quadratic background to the data by performing a least-squares fit. As many as nine peaks can be fit into a multiplet in this way. The program SKLN is a peak fitting program which fits a high-energy tail in addition to the low-energy tail and Gaussian of PEAKFIND. The input parameters to SKLN allow the fit of additional peaks into

---

[1] PEAKFIND and SKLN, Instructions for users. Mimeo. Ames, Iowa, Iowa State University of Science and Technology. A complete description of the fitting programs is presented in reference (43).

multiplets and the fitting of single peaks which were sometimes missed by the automatic peak search program. The data analysis was performed in three steps. First, plots of the spectrum to be analyzed were obtained. Then, using these plots, estimates of the FWHM and the energy slope and intercept were given to PEAKFIND as initial parameters. This step was repeated several times until good fits were obtained for the strong peaks by changing the initial estimates for the FWHM and skewness. Finally, those peaks not fit correctly by PEAKFIND were fit by SKLN using the appropriate parameters from good fits by PEAKFIND. Both programs gave precise values for the peak centroids, areas, full-widths at half-maximum, and the tailing parameters. In addition, these programs gave estimates of the errors in these quantities which could be used as a measure of the "goodness of the fit." Samples of fits using SKLN are shown in Figures 12 and 13. The first figure is a fit of the triplet at 880 keV 54 minutes after irradiation, and the second figure is the same region 345 minutes after irradiation. The two peaks at 890 keV were fit using the parameters (full-width at half-maximum and skewness) given by PEAKFIND for the 871 keV ^{94m}Tc peak.

To simplify the decay scheme analysis, energy values for the prominent peaks were determined to $\pm$ 0.1 keV. The 23 cc Ge(Li) detector was used in an ungated mode to count known calibration sources and then known calibration sources with the irradiated ruthenium. The spectrum was divided into "low" (100-1500 keV) and "high" (600-2500 keV) energy regions to simplify the analysis. For the low-energy region, ^{133}Ba,

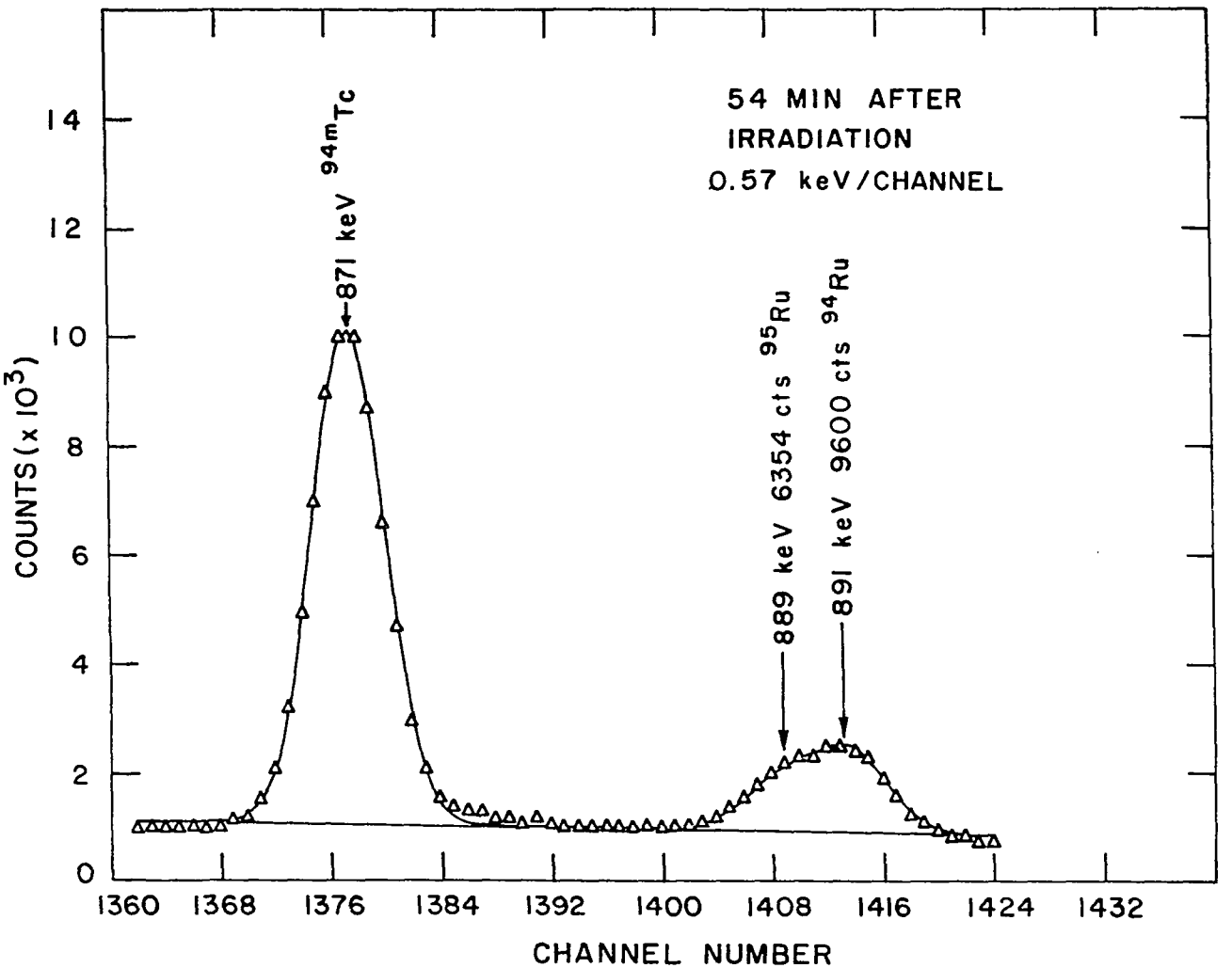

Figure 12. Sample computer fit to photopeaks

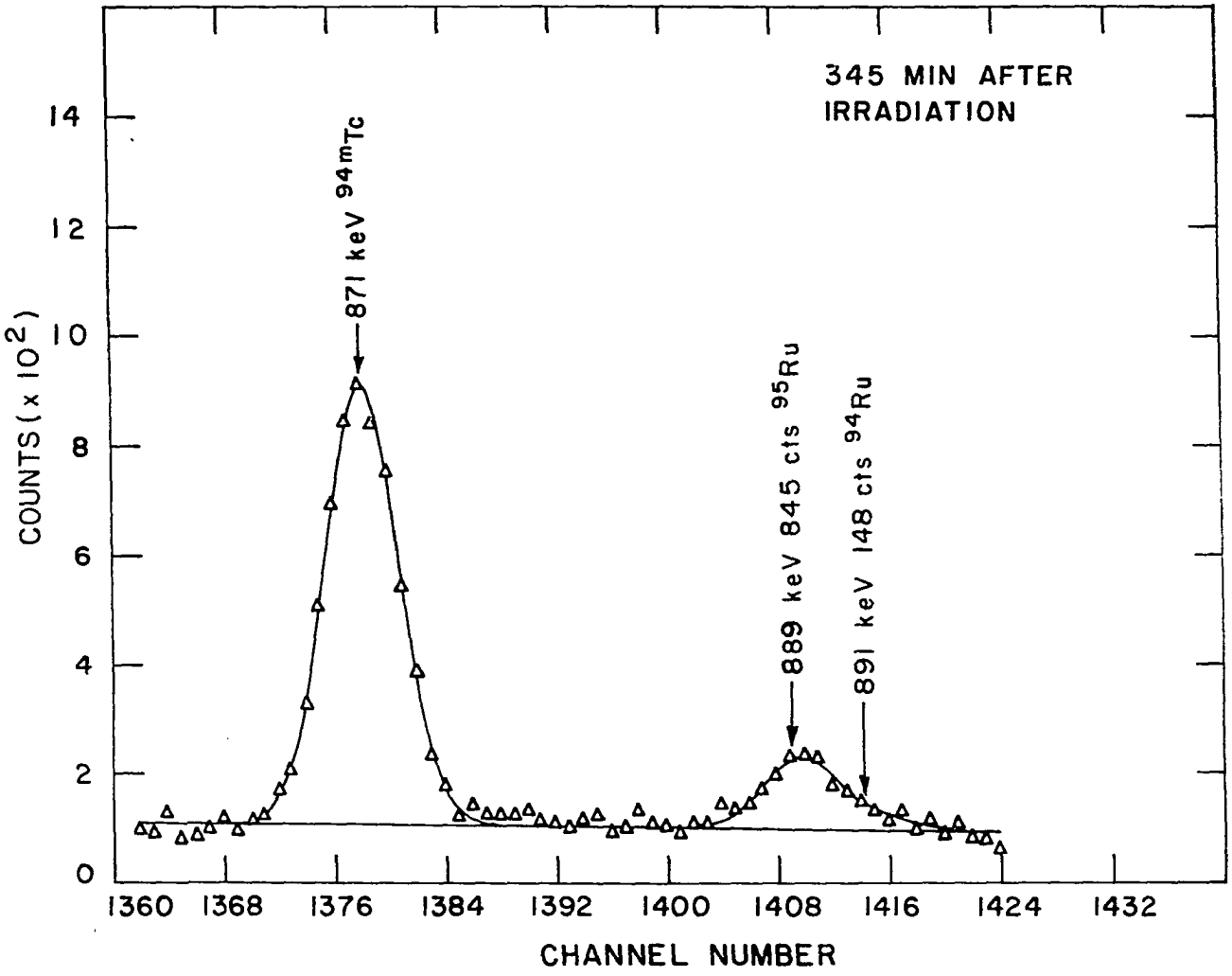

Figure 13. Sample computer fit to photopeaks. Note the different half-lives of the two components of the 890 keV peak by comparing with Figure 12

^{152}Eu, ^{110m}Ag, and ^{22}Na were used as calibration sources (44). For the high-energy region, ^{110m}Ag, ^{56}Co, and ^{226}Ra were used as calibration sources (44).

The energy-versus-channel number relation was fit by assuming a linear relationship and measuring deviations over the two regions from the accumulation with calibration sources only. The energy of a gamma ray with centroid in channel C can then be written:

$$E(C) = mC + b + \Delta(C),$$

where m and b are the slope and intercept constants which best fit the straight line and $\Delta(C)$ is the measured non-linearity. For this experiment, it was found that the linear constants could be chosen so the non-linearity over each region was less than .06 keV and could be neglected.

Using the combined calibration and irradiated ruthenium accumulations, peak centroids were determined using PEAKFIND. From this data, energies of the prominent peaks in the decay of ^{95}Ru were determined to $\pm$ 0.1 keV relative to the calibration source photopeaks. The energies of the less intense gamma rays were then determined from the irradiated ruthenium data, using the prominent ^{95}Ru gamma rays as the calibration lines. The uncertainties in the energies of these weaker transitions is typically $\pm$ 0.2 keV, although several have uncertainties as large as $\pm$ 0.5 keV.

The intensities of the ^{95}Ru gamma rays were calculated by dividing the peak area by the relative efficiency taken from Figure 9 for the Compton suppression system. Since the relative efficiency curves are

accurate to ± 5% and the area of most peaks has a relative error of approximately ± 2%, the error in the intensities of prominent peaks should be less than ± 10%. The error in the intensity of weaker peaks may be somewhat greater, depending on the counting statistics.

D. Results

1. Energies and intensities

Peak areas of the seven 40 minute runs were plotted on semi-log graph paper as a function of time to determine which gamma rays from the natural ruthenium sample belonged to the 99 minute ^{95}Ru decay. The decay curves for the intense 336 keV and the weak 889 keV transitions are shown in Figure 14. The decay curves for the other transitions are similar and are not shown. None of the competing activities have half-lives within ± 40 minutes of the ^{95}Ru activity, so all gamma rays which decayed with a half-life of 99 ± 10 minutes were assigned to the ^{95}Ru decay.

The energies and intensities (converted to absolute intensities as will be explained in Subsection 3.) obtained using techniques described in the last section are shown in Table 1. The energies listed for this work are the mean of several determinations. The intensities reported by Pinston et al. (26) are also given for comparison. The energy agreement between Pinston et al. and this experiment is ± 0.5 keV, or better, in all cases.

2. Coincidence data

The spectra which resulted from gating on the 336, 627, 1051, and

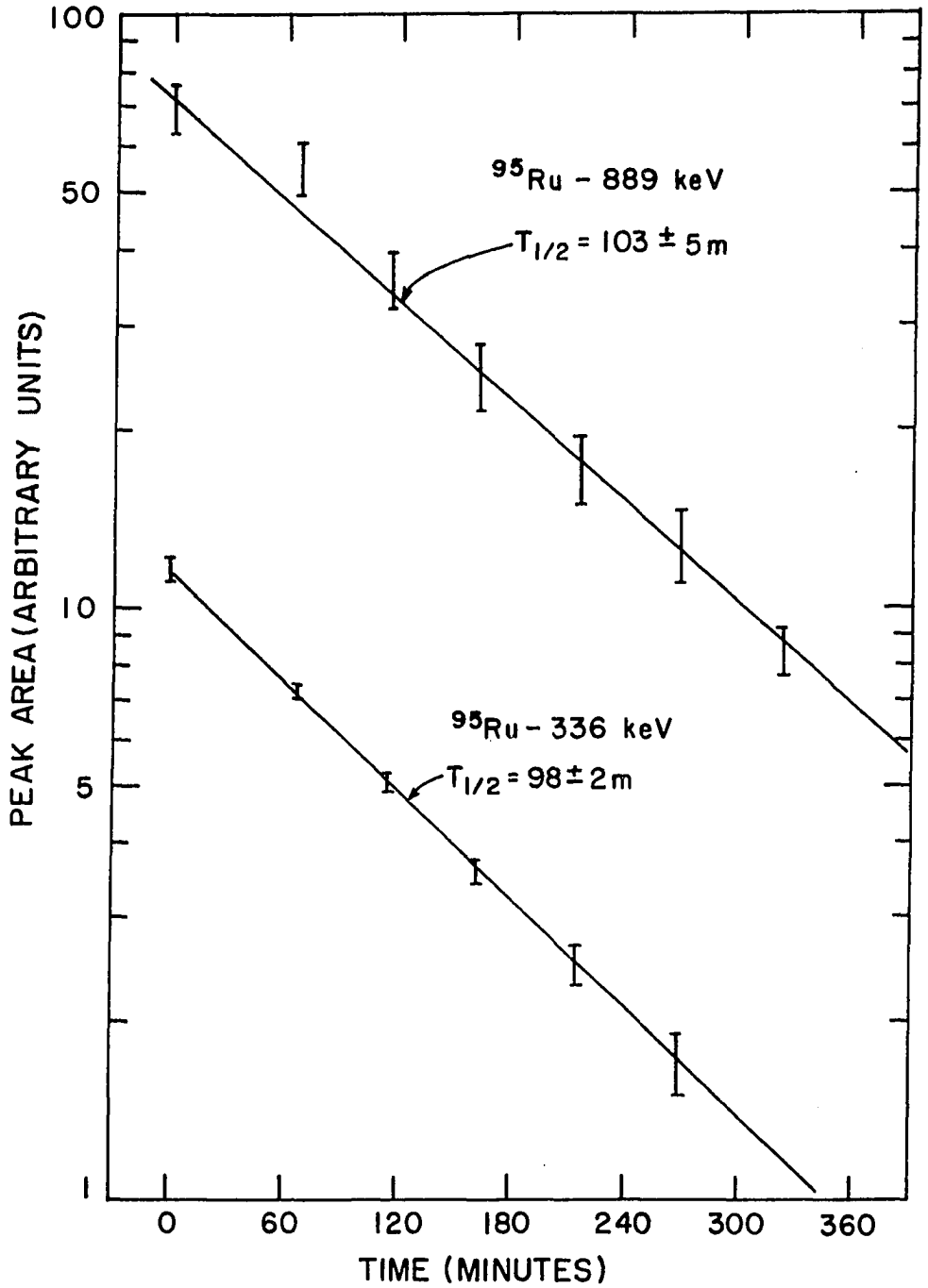

Figure 14. Decay of the 336 and 889 keV gamma rays from ^{95}Ru

Table 1. Gamma rays from the decay of ^{95}Ru

Transition Number	Energy (keV)	Intensity	Intensity[a]
1	290.32 ± 0.1	3.9 ± 0.4	3.5
2	301.00 ± 0.1	2.3 ± 0.2	1.8
3	336.42 ± 0.1	70.0 ± 7	70.5
4	551.59 ± 0.1	1.6 ± 0.2	1.7
5	591.43 ± 0.1	1.2 ± 0.1	1.0
6	626.82 ± 0.1	18.0 ± 2	14.0
7	652.79 ± 0.1	1.0 ± 0.1	0.7
8	735.0 ± 0.3	0.44 ± 0.04	b
9	748.49 ± 0.1	1.6 ± 0.2	b
10	806.25 ± 0.1	4.2 ± 0.4	2.9
11	818.96 ± 0.3	0.56 ± 0.06	b
12	842.12 ± 0.1	1.2 ± 0.1	0.8
13	888.69 ± 0.2	1.7 ± 0.2	b
14	990.12 ± 0.3	0.61 ± 0.06	b
15	1010.55 ± 0.3	0.68 ± 0.07	b
16	1050.68 ± 0.1	2.5 ± 0.2	1.5
17	1064.47 ± 0.2	0.70 ± 0.07	b
18	1096.75 ± 0.1	22.0 ± 2	15.0
19	1120.10 ± 0.2	0.85 ± 0.08	0.55

[a]The intensities of Pinston et al. (26) have been normalized to this experiment at 336 keV.

[b]Not seen.

Table 1. (Continued)

Transition Number	Energy (keV)	Intensity	Intensity[a]
20	1158.36 ± 0.1	1.4 ± 0.1	1.1
21	1178.69 ± 0.1	5.3 ± 0.5	3.4
22	1261.68 ± 0.3	0.32 ± 0.03	b
23	1339.75 ± 0.3	0.25 ± 0.02	b
24	1351.70 ± 0.5	0.44 ± 0.04	b
25	1354.70 ± 0.5	0.72 ± 0.07	1.1
26	1410.97 ± 0.3	2.4 ± 0.2	1.8
27	1433.47 ± 0.3	0.57 ± 0.06	b
28	1459.16 ± 0.2	2.2 ± 0.2	1.6
29	1541.64 ± 0.3[c]	0.22 ± 0.02	b
30	1562.23 ± 0.3[c]	0.15 ± 0.02	b
31	1785.36 ± 0.3	0.58 ± 0.06	0.8
32	1931.09 ± 0.3[c]	0.33 ± 0.03	b
33	1988.03 ± 0.3	0.70 ± 0.07	1.1
34	2046.98 ± 0.3	0.33 ± 0.03	b
35	2251.99 ± 0.3	0.35 ± 0.03	0.6
36	2324.54 ± 0.2	1.4 ± 0.1	1.5

[c]Not placed in the decay scheme.

1097 keV gamma rays are shown in Figures 15, 16, 17, and 18. For each of the coincidence experiments, the background spectrum was subtracted from the coincidence spectrum to yield the true coincident events. Ten counts have been added to each channel to display the negative fluctuations in the semi-log plots.

The results of the Ge(Li)-Ge(Li) coincidence experiments are summarized in Table 2. Those transitions indicated with an S were seen strongly in coincidence. This means they were enhanced in the coincidence spectrum compared to their relative intensity in the ungated singles spectrum. These gamma rays are probably involved in a direct cascade with the gating transition. Those transitions indicated with a W were seen weakly in coincidence. They are probably members of a cascade with several branches.

In Figure 15, a 336 keV gamma ray appears in the 336 keV gated spectrum. This can be explained by noting that the 336 keV transition is located on the sharply rising portion of the Compton edge of the 511 keV annihilation peak. The background window had to be positioned on this rising background, and hence could not account for all the background counts seen in the 336 keV gating channel. This explanation also accounts for the other transitions identified as background lines in Table 2. All the levels which these gamma rays depopulate are fed directly by the positron decay from ^{95}Ru, ^{95}Tc, and ^{95}Tc.

3. Decay scheme

The decay scheme of ^{95}Ru was constructed using the energy and

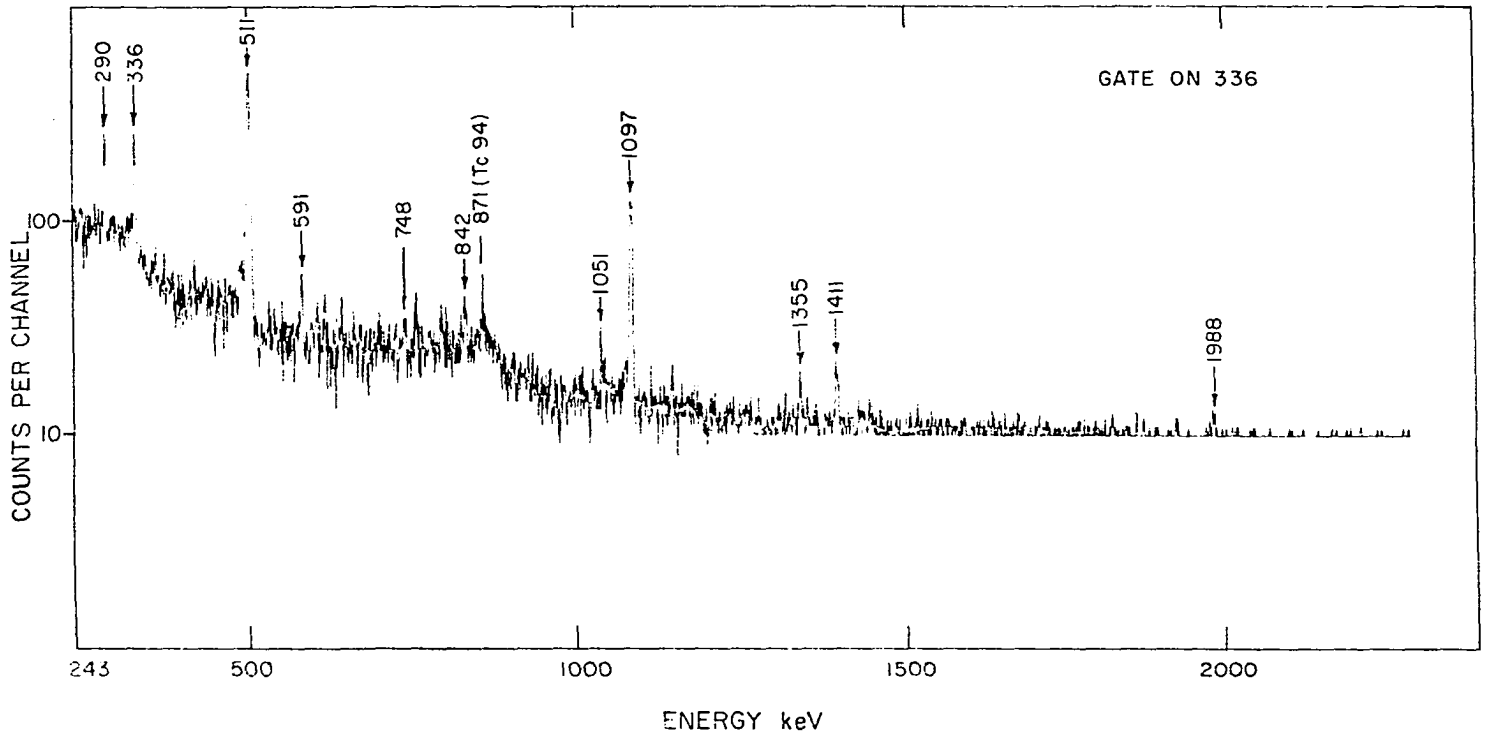

Figure 15. Ge(Li)-Ge(Li) coincidence spectrum of ^{95}Ru gamma rays gated by the 336 keV gamma ray

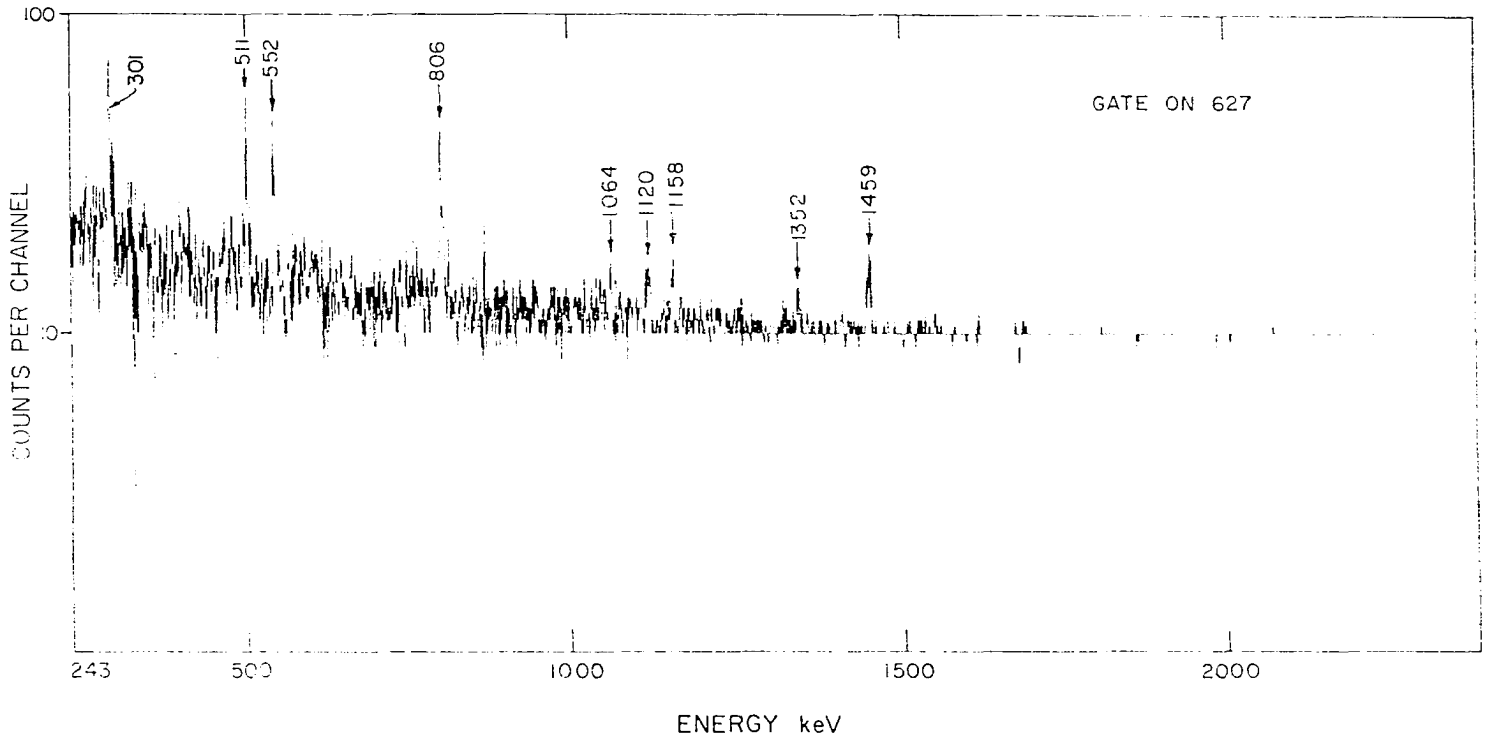

Figure 16. Ge(Li)-Ge(Li) coincidence spectrum of ^{95}Ru gamma rays gated by the 627 keV gamma ray

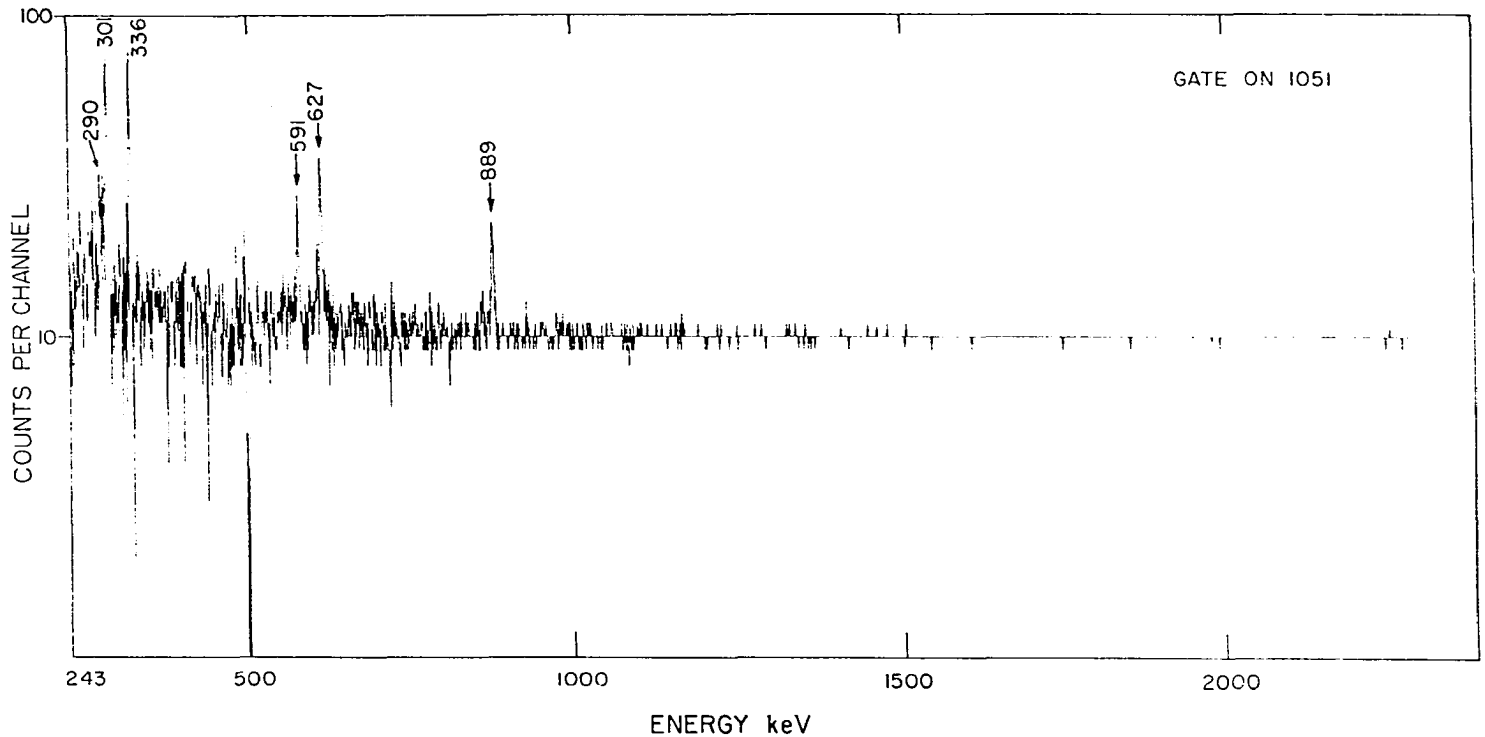

Figure 17. Ge(Li)-Ge(Li) coincidence spectrum of ^{95}Ru gamma rays gated by the 1051 keV gamma rays

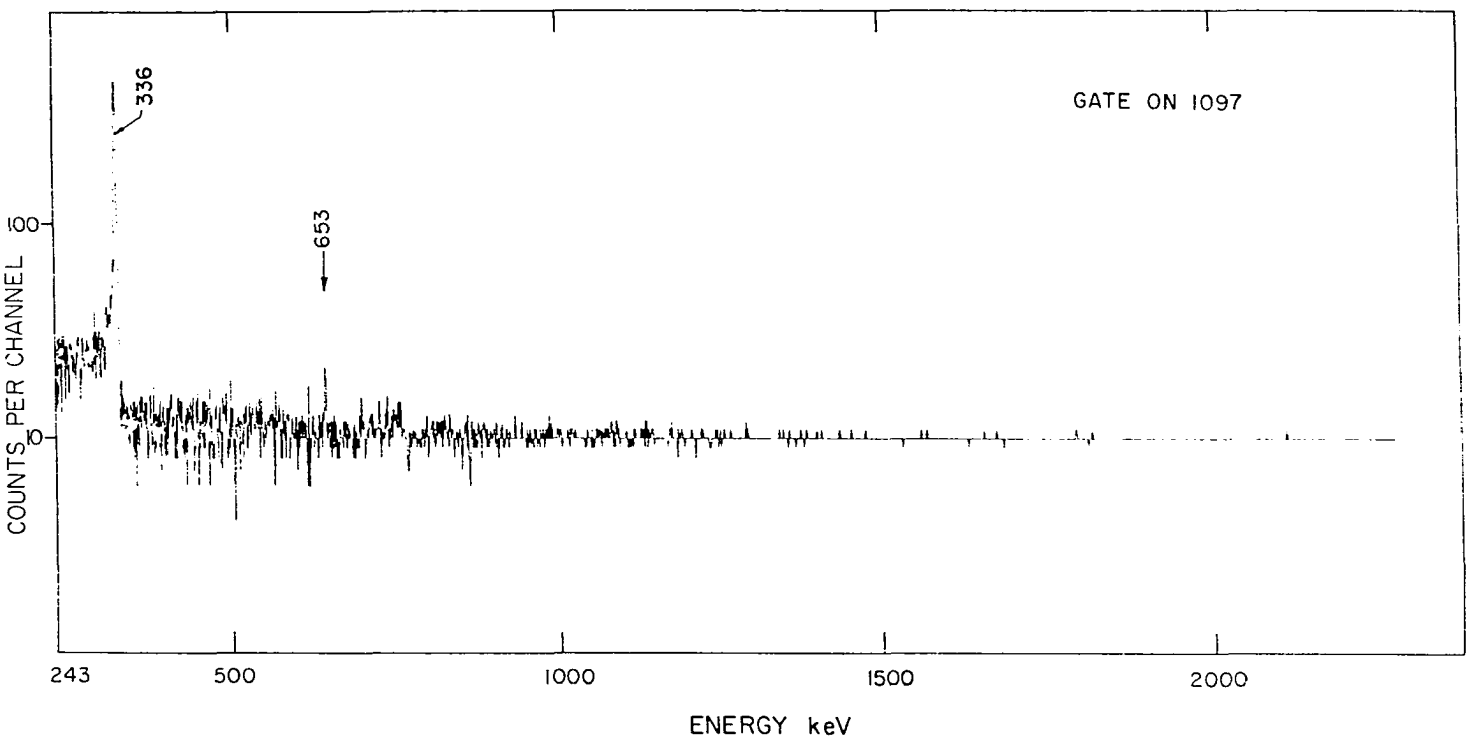

Figure 18. Ge(Li)-Ge(Li) coincidence spectrum of ^{95}Ru gamma rays gated by the 1097 keV gamma rays

Table 2. Summary of coincidence spectra

Energy of coincident gamma ray (keV)	Energy of gating gamma rays (keV)			
	336	627	1051	1097
290	S		W	
301		S	S	
336	B		W	S
552		S		
591	S		S	
627	B		W	
653	W			S
748	W			
765[a]	B			
806	W	S		
842	S			
871[b]	B			
889			S	
1051	W			
1064		S		
1097	S			
1120		S		
1158	W	S		
1352		S		
1355	S			
1411	S			
1459	W	S		
1988	S			

S -- strong W -- weak B -- background or chance

[a] From the decay of ^{95}Tc.

[b] From the decay of ^{94}Tc.

intensity measurements of the present experiment along with the Ge(Li)-Ge(Li) coincidence data. Table 3 lists the energy sums which are relevant to the construction of the decay scheme. In the case where there was no coincidence data, or when the coincidence data was inconclusive, the energy sums were used to place the gamma rays in cascade. The resulting decay scheme is shown in Figure 19.

The placement of all levels except those at 990, 1049, 2251 keV was verified by the coincidence data. The two levels at 990 and 1049 keV are dotted in as tentative because they are placed on the basis of only one energy sum. The level at 2252 keV is more definite because of the ground state transition depopulating this level.

According to the work of Pinston et al. (26), the ground state of ^{95}Tc is not fed by the beta decay of ^{95}Ru. The relative intensities discussed in Section II., B. can then be converted into absolute intensities by requiring the sum of the intensities of transitions feeding the ground and isomeric states to be equal to 100%. The total positron plus electron capture branching ratios can be calculated from the imbalance of electromagnetic transitions into and out of each level. Log(ft) values were then calculated using these branching ratios and the nomogram from reference (28). The levels in Figure 19 are labelled with the per cent decay and the log(ft) values.

Of the 36 gamma rays observed, those at 1542, 1562, and 1931 keV were not placed in the decay scheme. Since they were not seen in coincidence with either the 336 or 627 keV gammas, they are probably direct transitions to either the ground or isomeric states.

Table 3. Energy sums

Level Energy	Transition Number (Table 1) or Level Energy		Energy Sum
626.8	1 + 3	=	626.74 ± 0.14
	13 + (38.9)	=	927.59 ± 0.22
927.8	2 + 6	=	927.82 ± 0.14
	5 + 3	=	927.85 ± 0.14
	21	=	1178.69 ± 0.1
1178.6	12 + 3	=	1178.54 ± 0.14
	4 + 6	=	1178.41 ± 0.14
	27	=	1433.47 ± 0.3
1433.2	10 + 6	=	1433.07 ± 0.14
	18 + 3	=	1433.17 ± 0.14
	23 + 3	=	1676.17 ± 0.3
1676.3	9 + (927.8)	=	1676.29 ± 0.14
	25 + 3	=	1691.12 ± 0.5
1691.3	17 + 6	=	1691.28 ± 0.2
	26 + 3	=	1747.39 ± 0.3
1747.0	11 + (927.8)	=	1746.76 ± 0.3
	19 + 6	=	1746.92 ± 0.2
	20 + 6	=	1785.18 ± 0.14
1785.2	8 + 15 + (38.9)	=	1785.45 ± 0.4
	31	=	1785.36 ± 0.3
	24 + 6	=	1978.52 ± 0.5
1978.5	16 + (927.8)	=	1978.48 ± 0.14
	34 + (38.9)	=	2085.88 ± 0.3
2086.0	28 + 6	=	2085.98 ± 0.22
	7 + (1433.2)	=	2085.99 ± 0.14
	35	=	2251.99 ± 0.3
2251.9	22 + 14	=	2251.80 ± 0.42
	33 + 3	=	2324.45 ± 0.3
	36	=	2324.54 ± 0.2

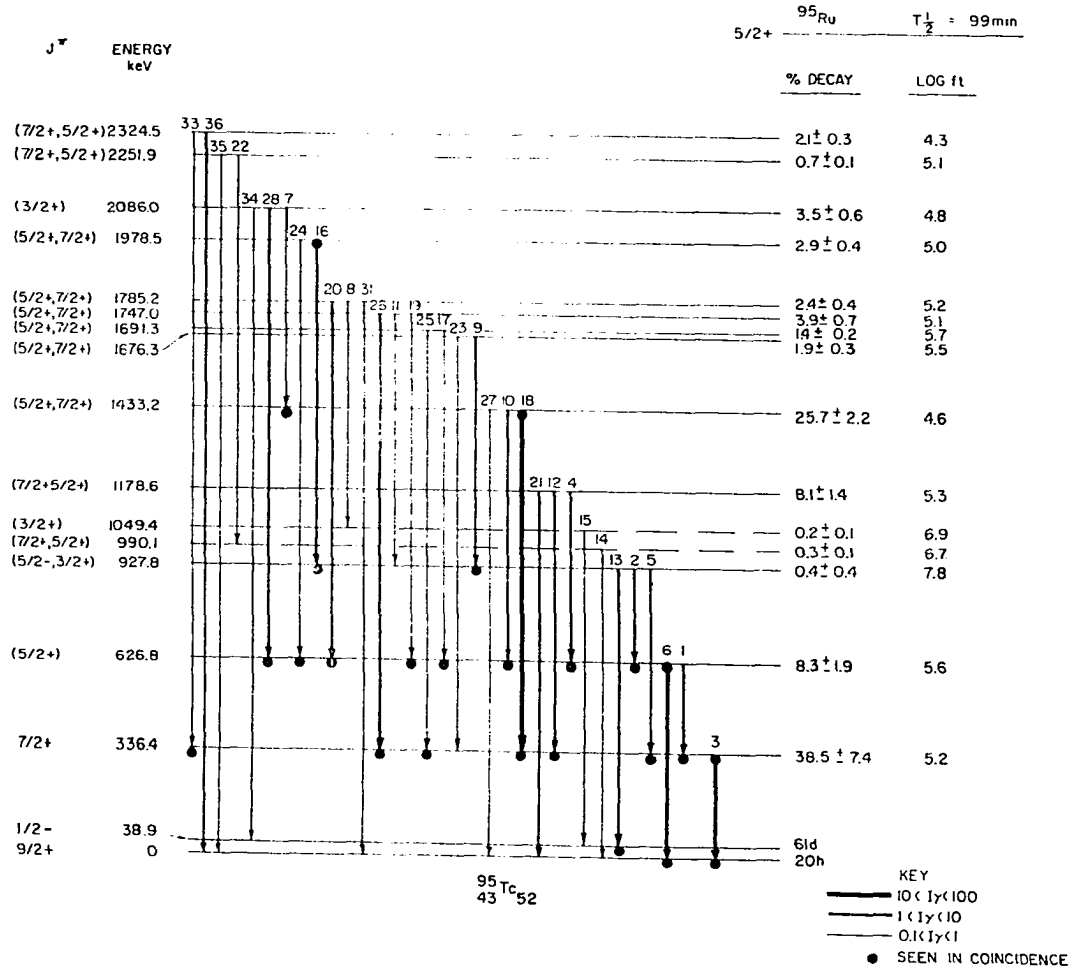

Figure 19. Decay scheme for ^{95}Ru. The numbering of transitions corresponds to their order in Table 1. The coincidence results are shown by dots, at the start of an arrow to label a gating transition and at the tip to indicate an enhanced line

First forbidden decays in this mass range have log(ft) $\geq$ 8 (28); so the beta decay branches with log(ft) $\leq$ 7 are assumed to be allowed transitions. Since $J^{\pi} = 5/2^{+}$ for the ground state of ^{95}Ru, allowed beta decay can populate positive parity states with J = 3/2, 5/2, or 7/2. Because only M1, E1, and E2 gamma rays should have observable intensity, a direct transition to the $9/2^{+}$ ground state eliminates the $3/2^{+}$ possibility. Similarly, the presence of a gamma ray feeding the $1/2^{-}$ level excludes the $5/2^{+}$ and $7/2^{+}$ assignments.

The M1 multipolarity (25) of the transition to the $9/2^{+}$ ground state indicated $J^{\pi} = 7/2^{+}$ for the 336 keV level. The next level at 627 keV has an allowed log(ft) value and feeds the 336 keV level with a moderately intense transition. The level could be a $5/2^{+}$ or $7/2^{+}$. However, its intensity to the ground state is only 1/5 that of the 336 keV level, and it is probably a $5/2^{+}$. This assignment also agrees with neighboring odd-Z nuclei ^{93}Nb (45, 46, 47) and ^{99}Tc (48). The 927 keV level decays to $5/2^{+}$, $7/2^{+}$, and $1/2^{-}$ states, so $J^{\pi} = 5/2^{-}$ or $3/2^{+}$ assignments are possible. The uncertainty in the net gamma feeding is too large to determine a conclusive log(ft), however the strong gamma feeding from higher energy positive parity states in competition with transitions to lower states suggests E1 multipolarity and the choice of $5/2^{-}$. Probable spin and parity assignments proposed for the levels above 928 keV are based on the general arguments given above. Where both $5/2^{+}$ and $7/2^{+}$ are possible, the more probable value, as determined by the relative intensities of the transitions feeding the low-lying states, is listed first.

Before leaving this section, a comment should be made about the levels at 928 and 1049 keV. The beta branching fractions to these levels were determined from the differences of small numbers. Therefore, the uncertainties are too large to yield accurate log(ft) values, so the type beta decay cannot be assigned. The tentative assignments given these levels is based almost entirely on the spins and parities of levels which they feed.

4. Discussion

The decay scheme shown in Figure 19 generally agrees with the one proposed by Pinston et al. (26) (Figure 4). The earlier decay scheme had no gamma rays feeding the $1/2^-$ level. Three of the fifteen new gamma rays seen in this experiment are identified as transitions to this level: the 2047, 1011, and 889 keV transitions. Their existence helps determine the probable spins and parities of levels at 2086, 1049, and 928 keV. The 1085 keV level de-exciting through a 749-336 keV cascade proposed by Pinston et al. has been eliminated because the intensity of the 749 keV gamma ray in the spectrum gated by the 336 keV transition was too small to have it feeding the 336 keV level. Instead, the 749 keV transition is placed as de-exciting the 1676 keV level through the 749-591-336 keV cascade. On the basis of its intensity in the coincidence spectrum gated by the 627 keV transition, the 1158 keV gamma ray has been moved from 2086-928 to 1785-627. The present work places new levels at 990, 1094, 1676, and 1691 keV.

Kim et al. (27) reported levels at 651, 670, 960, 1087, 1213,

1281, 1332, 1415, 1618, and 1636 keV in addition to the levels seen in this experiment. They reported no levels with an energy greater than 1650 keV and they did not see levels at 990 and 1049 keV. The existence of a level at 670 keV once again raises the question of a possible 336-336 keV coincidence. However, the gamma-ray singles data shows no evidence of a 672 keV gamma. Again, since different selection rules apply to reaction and decay experiments, all of the levels should not be seen in both experiments.

III. DECAY OF ^{103}Tc

The recent reaction work of Diehl et al. (34) and Nolen et al. (35) has shown ^{103}Ru to have a large number of levels not seen in the decay work of Kienle et al. (31). The levels which Kienle et al. reported to be fed by the beta decay of ^{103}Tc at 135 and 350 keV have been assigned spins and parities ($3/2^+$, $5/2^+$) and ($5/2^+$) respectively by Diehl et al. (both assignments are tentative). Since many other positive parity levels with J = 3/2, 5/2, and 7/2 were seen in the reaction studies, one would expect a more complex ^{103}Tc beta decay than has been reported.

The work of Brandi et al. (32) and Gabsdil (33) indicates that the ~210 keV transition which they see decay with a half-life of 1.7 ± 0.3 milliseconds is not in coincidence with a 135 keV gamma ray. This implies that this 210 keV gamma ray is not the same as the 215 keV gamma ray which Kienle et al. place as feeding a 135 keV level. If the level at 210 keV seen by Diehl et al. is the isomeric level of Brandi et al. and Gabsdil, the spin and parity assignment of $7/2^+$ is inconsistent with the $5/2^+$ assignment for the ground state since a 210 keV M1 or E2 transition would not have a millisecond lifetime.

This chapter discusses the use of Ge(Li) detectors, both singly and in coincidence spectrometers, to resolve the inconsistencies pointed out above.

A. Source Preparation

Sources of radioactive ^{103}Tc were produced by the ^{104}Ru(γ,p)^{103}Tc

reaction using the same irradiation facility described in Section II. However, the 50 second ^{103}Tc activity had to be counted as soon as possible after irradiation. Following irradiation, the samples were placed into a pneumatic tube which connects the synchrotron with a counting room in the reactor building 1/5 mile away. The time elapsed from the end of the irradiation period until the counting was begun was typically 50 seconds, or one ^{103}Tc half-life.

Two types of samples were used in this experiment. Initial studies were done with the 2.4 gram natural ruthenium metal target used in the ^{95}Ru study. For this experiment, the target was divided into three smaller samples so that successive runs could be taken without the buildup of longer lived activities. Although several gamma rays were seen to have a half-life of 50 seconds, the complexity of the spectrum due to other activities (Figure 10) made the data analysis very difficult. In addition, the possible production of the 50 second ^{93}Ru (4) activity through the ^{96}Ru(γ,3n) reaction made an unambiguous assignment to ^{103}Tc impossible.

The second sample used was 125.3 milligrams of powdered ruthenium metal enriched to 98.2% in ^{104}Ru (principal contaminants: ^{102}Ru--1.3%, ^{101}Ru--0.3%, ^{100}Ru--0.1%, ^{99}Ru--0.1%) borrowed from Oak Ridge National Laboratory. This sample was encapsulated in an aluminum can and irradiated in the same way as the natural ruthenium samples. It was then placed in a polyethylene transfer rabbit and sent to the reactor as described above. To minimize delays and loss of the powdered sample, the sample was left in the aluminum can and in the transfer rabbit

during counting.

The only competing activity which was hard to distinguish from 50 second ^{103}Tc was the 60 second ^{25}Na activity produced in the ^{28}Al(γ,3p) reaction. This isotope has recently been studied by Jones, Becker, McDonald, and Poletti (49) and the gamma rays associated with this decay are known.

B. Instrumentation

1. Gamma-ray singles measurements

Several Ge(Li) detectors were used for energy and intensity measurements. For the initial studies with the natural ruthenium samples, a 60 cc Ge(Li) detector with 3.1 keV FWHM resolution at 1.332 MeV was used. During data accumulations, pulses from the detector's preamplifier were amplified by a commercial "active filter" amplifier and recorded in a 4096-channel pulse height analyzer. Pulse shaping time constants and pole-zero cancellation were adjusted to maximize the resolution.

This same detector arrangement was used on the initial studies of the enriched sample. Since the Ge(Li) detector is sensitive to charged particles of all types, a 1/4 inch lucite beta absorber was placed between the sample and detector to reduce the beta background. However, because of the large number of closely spaced doublets, a 6 cc Ge(Li) detector with 2.5 keV FWHM resolution at 1.332 MeV was used for final energy and intensity measurements. The relative efficiency of this detector as a function of energy is shown in Figure 20. This was measured using ^{133}Ba and ^{226}Ra as sources (as was explained in

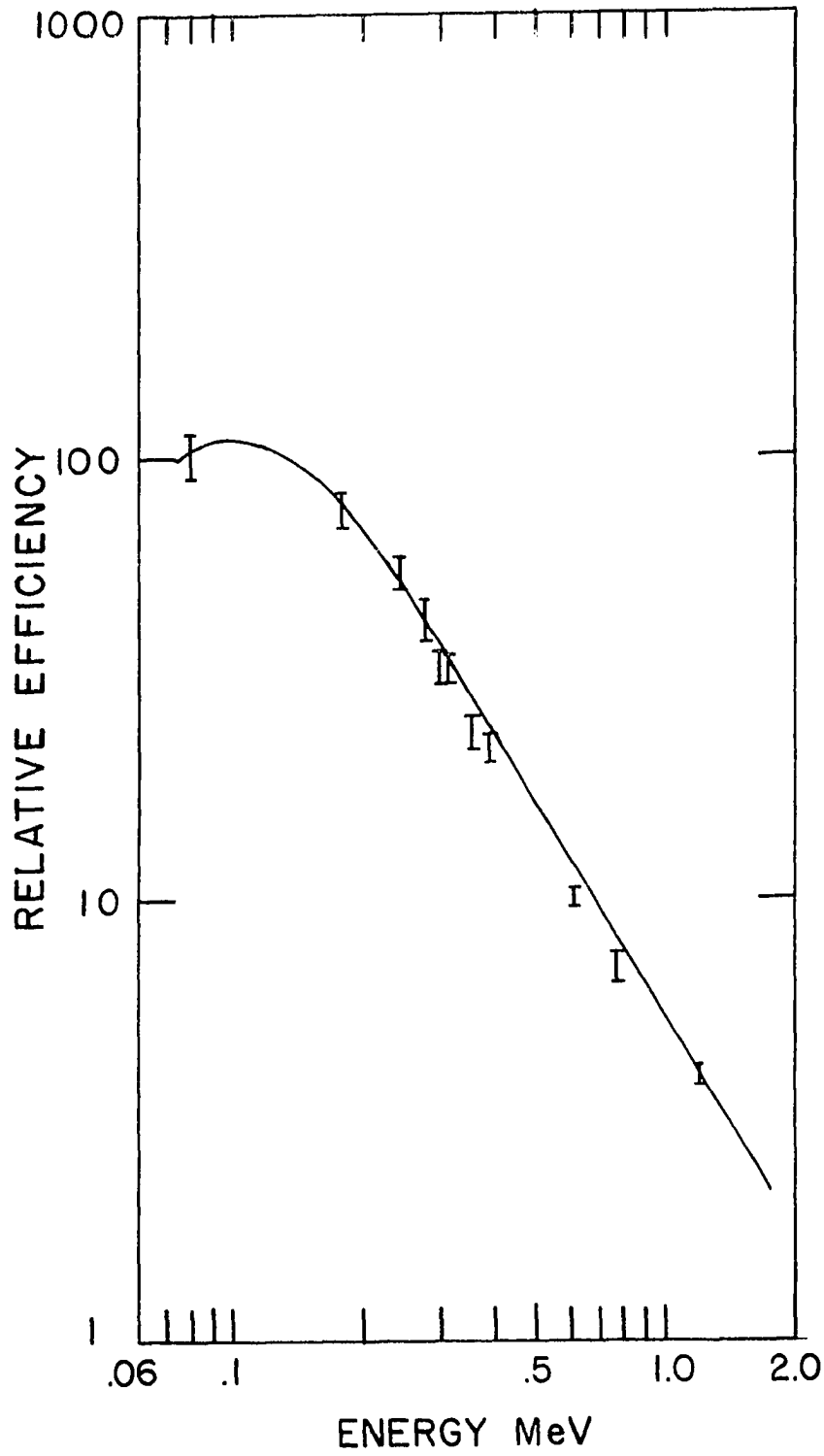

Figure 20. Photopeak efficiency versus gamma-ray energy for the 6 cc Ge(Li) detector

Section II.), for which accurate energies and intensities are known.

From the initial studies with the 60 cc detector, it was determined that there were no transitions with an energy greater than 1200 keV which could be assigned to the 50 second ^{103}Tc decay. Thus the gain and zero settings of the amplifier-analyzer system were adjusted so gamma rays with energies between 10 and 1200 keV could be studied. A typical spectrum taken with the 6 cc detector is shown in Figures 21 and 22. Gamma rays which have been assigned to the ^{103}Tc decay are labelled by their energy to the nearest keV. Those gamma rays which belong to activities from contaminants or the aluminum can are labelled by both their energy and origin. The assignment of the gamma rays is explained in Section III., C.

2. Gamma-ray coincidence measurements

The number of closely spaced doublets in the decay of ^{103}Tc requires a study with a Ge(Li)-Ge(Li) coincidence spectrometer. The same electronics were used in this experiment as described in Section II., B. and as shown in Figure 11. There were two changes made for this coincidence experiment. First, a 48.4 cc Ge(Li) detector with 3.1 keV resolution FWHM at 1.332 MeV was used as the gating detector and a 40 cc Ge(Li) detector with 2.9 keV resolution was used to record the coincidence spectrum. The second change was the addition of two more single channel analyzers in the gating circuit. This allowed the simultaneous recording of coincidences with three peaks and a background by routing the quadrants of the analyzer. As described in Section II., B., narrow windows (approximately 5 keV wide) were set on the peaks of

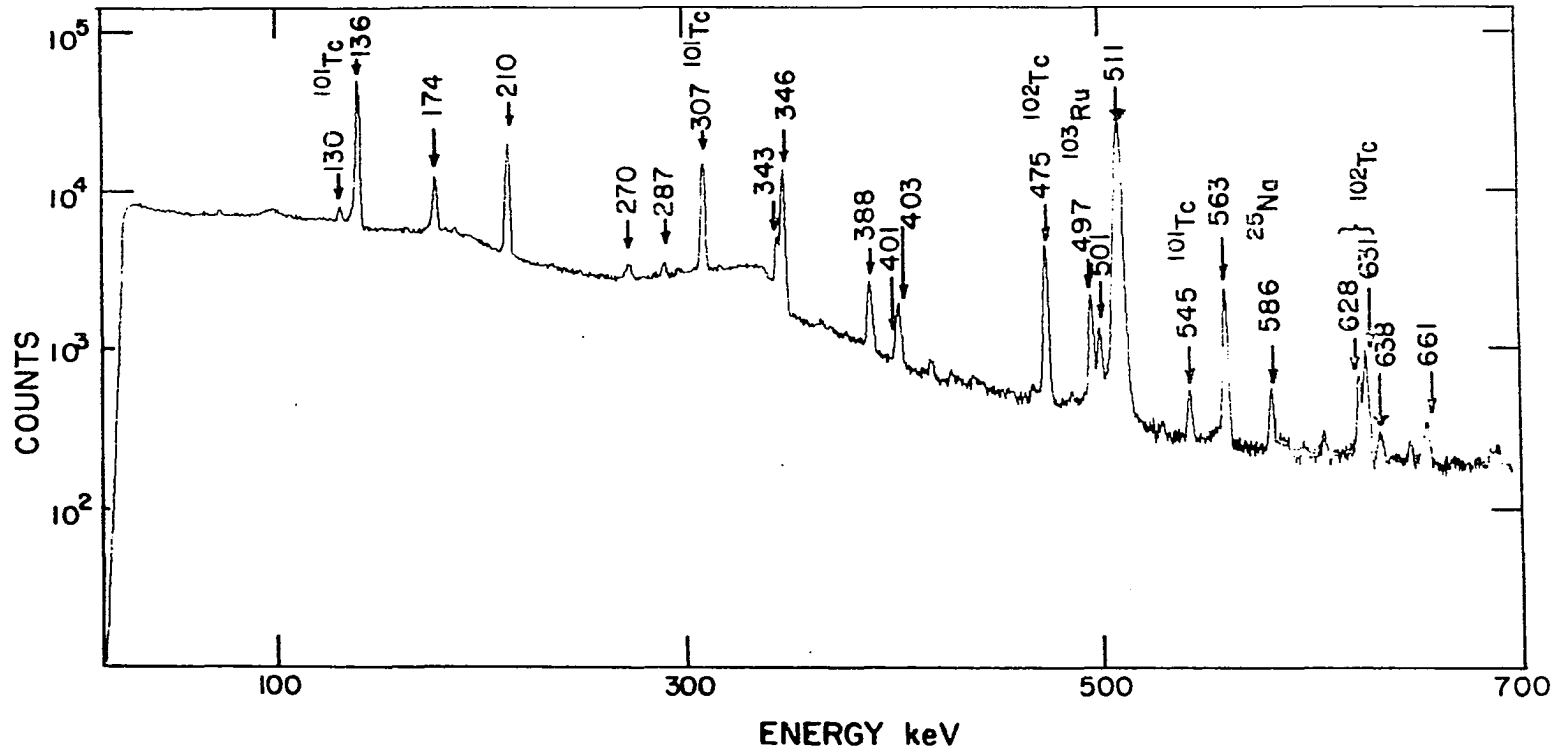

Figure 21. Low-energy portion of ^{103}Tc spectrum taken with 6 cc detector

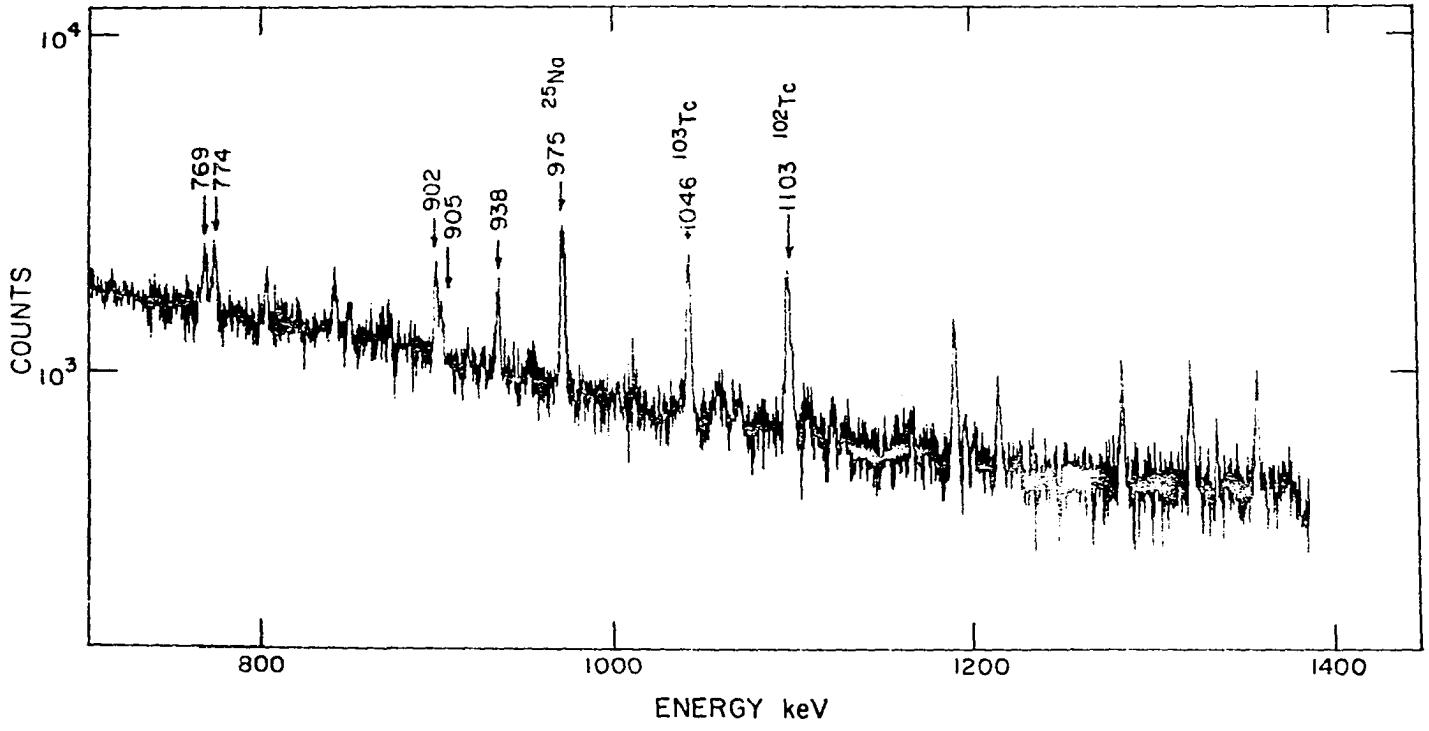

Figure 22. High-energy portion of ^{103}Tc spectrum taken with 6 cc detector

interest and a flat portion of the background near these peaks. The spectrum from the gating detector and the placement of these windows is shown in Figure 23.

Coincident spectra were recorded for the 136, 174, 210, 346, and 563 keV gamma rays from the decay of ^{103}Tc. For the first three transitions, the sample was irradiated for three minutes and coincidence data taken for two minutes. This cycle was repeated eight times. For the 346 and 563 keV transitions, the same cycle was repeated only three times. A single background spectrum was recorded for the 136, 174, and 210 keV gamma rays, since the background is nearly the same for these three transitions (Figure 23). Individual backgrounds were recorded for the 346 and 563 keV gamma rays by setting two of the single channel analyzers on flat portions of the background near the respective peaks.

To maximize the counting rate, the two Ge(Li) detectors were placed as close together as possible, and no lead was placed between the detectors. A spurious peak in each coincidence and background spectrum was produced by the Compton scattering from one detector into the other of the intense 511 keV annihilation radiation from the positron decay of the irradiated aluminum can. If, for example, the Compton scattered photon has an energy of 136 keV, a coincident peak at 511-136 keV will appear in the coincidence spectrum gated by the 136 keV signals. This peak will be broader than the normal spectral peaks because the gating detector will signal a coincidence for Compton scattered photons of energy 136 $\pm$ 2.5 keV due to the finite width of the window.

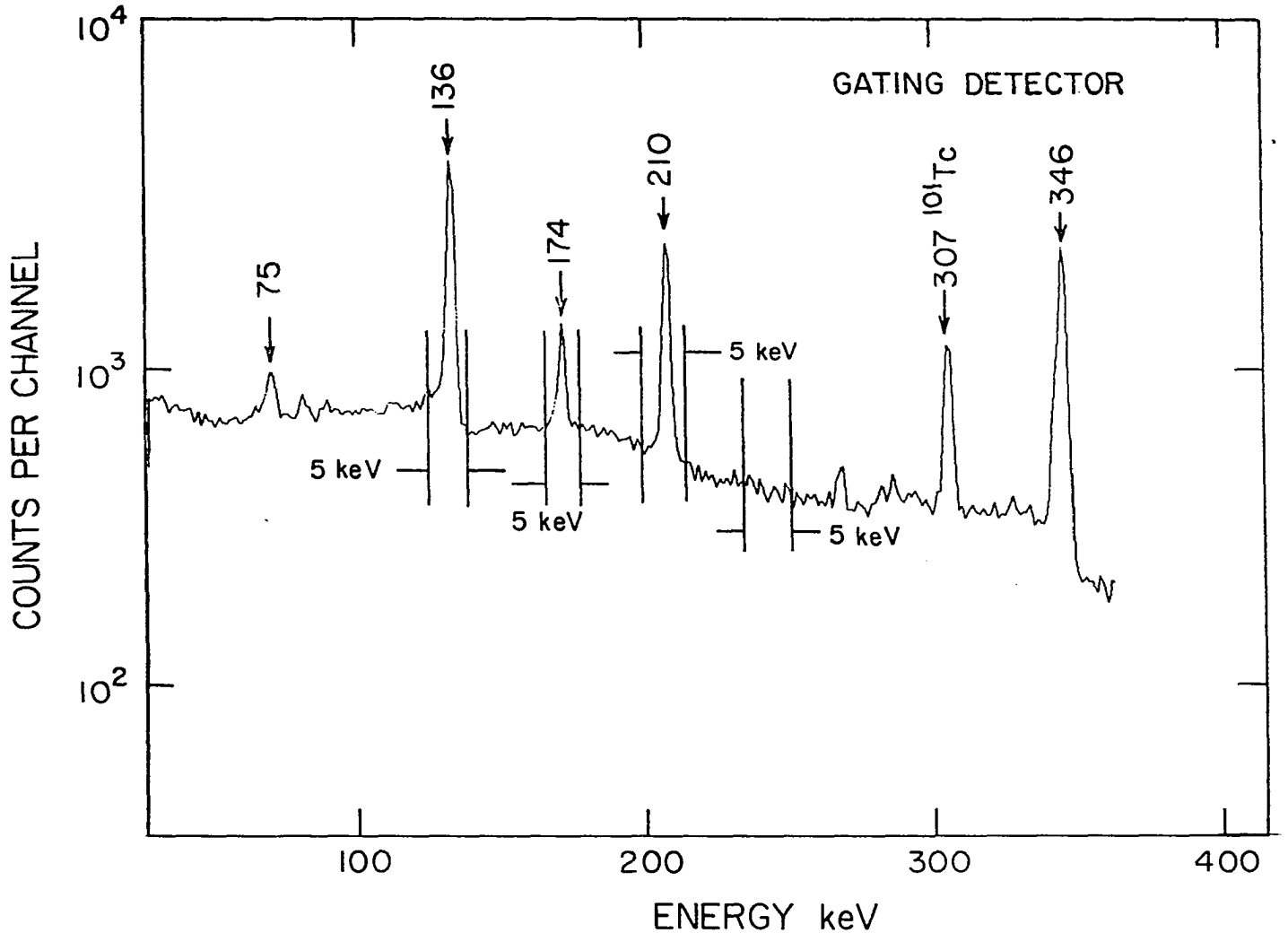

Figure 23. Spectrum in gating detector showing the placement of the single channel analyzer windows

C. Data Analysis

Both the natural ruthenium sample and the enriched sample were studied with the Ge(Li) detectors described earlier. Two types of studies were done to determine which gamma rays belonged to the 50 second ^{103}Tc decay. Using the 60 cc detector, samples which had been irradiated for 2 minutes were counted for 40 seconds into all 4096 channels of the analyzer memory. These data were then read onto magnetic tape, a process which takes 32.4 seconds for the entire 4096 channels. This cycle was repeated four more times using the analyzer's autocycle mode and then the sample was irradiated again. Six samples were irradiated and counted in this way, giving a total of 30 data sets. These 30 data sets were reduced to 5 by adding the corresponding data sets of each irradiation together. The output of a 60 cycle pulser was used to determine the analyzer livetime for each of the data sets by feeding this output into the test input of the detector's preamplifier and integrating the area of the resulting peak in the singles spectrum. Both the natural ruthenium sample and the enriched sample were studied in this way.

To eliminate the 32 seconds required for each readout of the analyzer memory, a second set of experiments was done with the enriched sample. Following a 4 minute irradiation, successive 1 minute accumulations were stored in each quadrant of the analyzer memory by hand-switching the memory location. This process was repeated for a total of four irradiations. The first and third 1 minute accumulations (corresponding to quadrants 1 and 3 of the analyzer memory) are shown in Figure

24. The peaks labelled with energy only have a 50 second half-life and have been assigned to the decay of ^{103}Tc. A similar experiment was done with 2 minute irradiations and 40 second accumulations. Decay curves from this data are shown in Section III., D..

Peak positions and areas for the two studies described above were calculated using the computer codes described in Section II., C. In addition, accurate energies and relative intensities were determined as discussed in that section. In this case, ^{57}Co, ^{22}Na, ^{133}Ba, and ^{226}Ra were used for the energy calibration (44).

D. Results

1. Energies and intensities

Peak areas (corrected for differences in analyzer livetime) were plotted on semi-log graph paper as a function of time for each of the peaks seen in the studies mentioned above. The decay curves for the doublet at 346 keV are shown in Figure 25 and the decay curves for the weaker 389 and 774 peaks are shown in Figure 26. The decay curves for the other transitions are similar and are not shown.

The energies and relative intensities obtained using techniques described previously are listed in Table 4. The gamma rays at 75, 216, 351, 365, and 427 keV were too weak in the singles spectrum (Figures 21 and 22) to be analyzed. They were enhanced in the coincidence spectrum and were assigned energies by using the prominent peaks in the coincidence spectrum as a calibration. Similarly, the peaks at 172, 487, 555, and 638 keV are weak members of multiplets which could not be resolved in the singles data but appeared enhanced in the coincidence

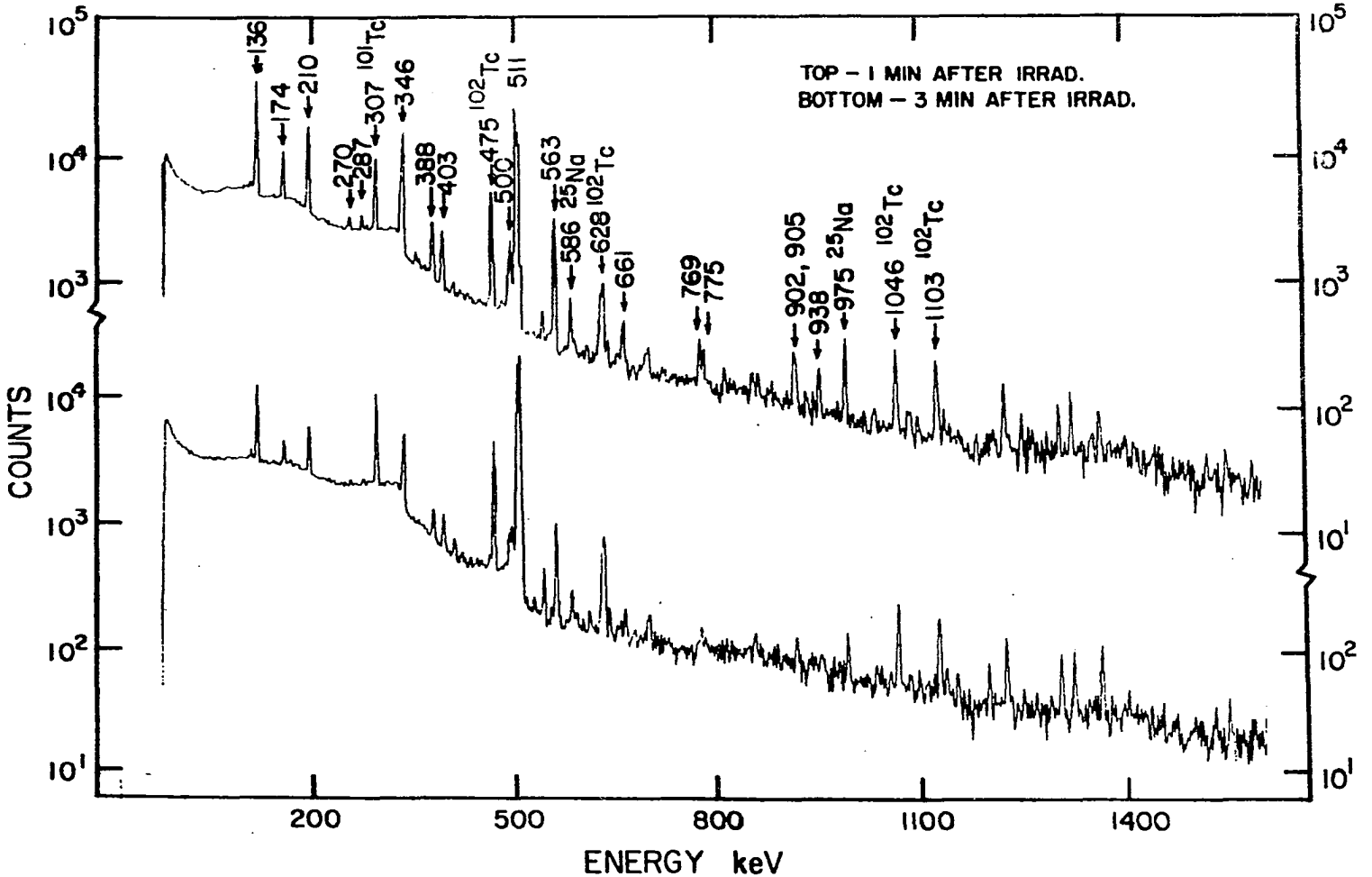

Figure 24. Two successive spectra showing the decay of the 50 second ^{103}Tc activity

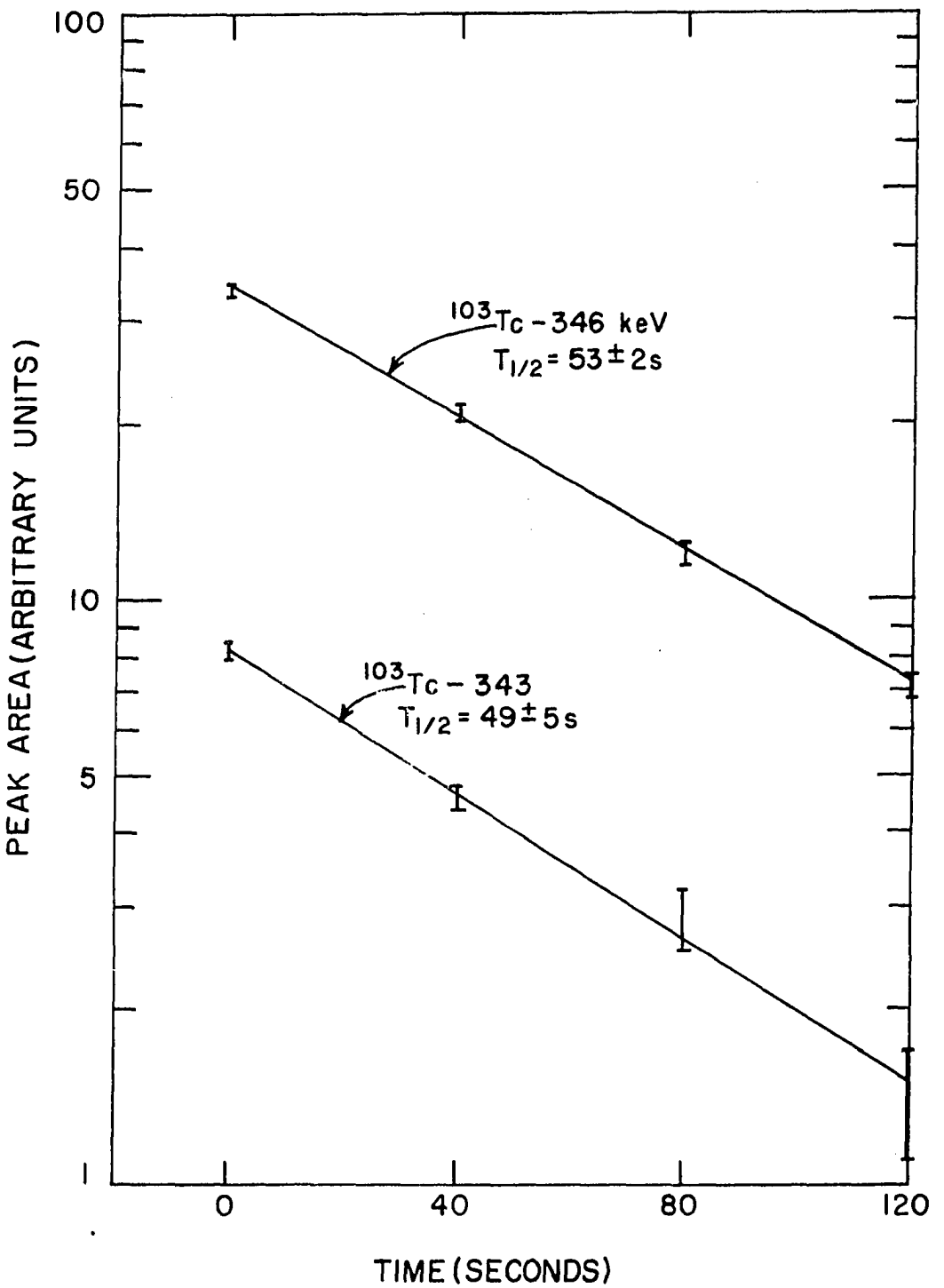

Figure 25. Decay of the 343 and 346 keV gamma rays of ^{103}Tc

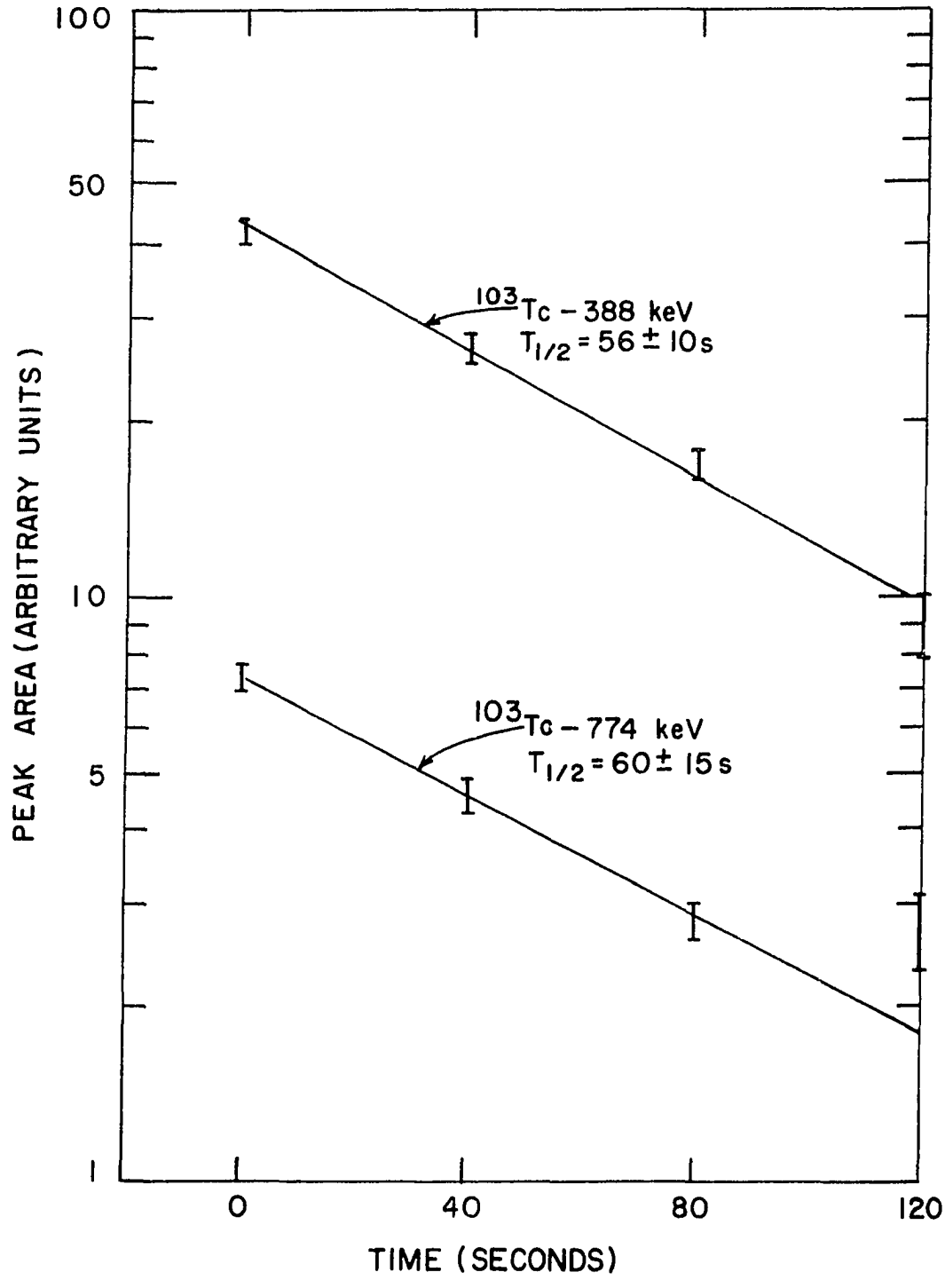

Figure 26. Decay of the 388 and 774 keV gamma rays of ^{103}Tc

Table 4. Gamma rays from the decay of ^{103}Tc

Transition Number	Energy (keV)	Relative Intensity
1	74.84 ± 0.3[a]	<1
2	136.00 ± 0.1	100
3	172.00 ± 0.5	1.2 ± 0.5
4	174.20 ± 0.1	17 ± 2
5	210.25 ± 0.1	58 ± 6
6	216.40 ± 0.5[a]	<1
7	269.63 ± 0.3	3.0 ± 0.5
8	287.22 ± 0.3	3.3 ± 0.5
9	343.28 ± 0.3	20 ± 2
10	346.18 ± 0.1	88 ± 8
11	351.23 ± 0.5[a]	<1
12	364.87 ± 0.5[a]	<1
13	388.48 ± 0.3	13 ± 2
14	401.43 ± 0.3[b]	4.0 ± 0.8
15	402.97 ± 0.3	12 ± 1
16	426.70 ± 0.5[a]	<1
17	487.25 ± 0.5[c]	
18	500.80 ± 0.3	12 ± 1

[a]Weak, seen only in coincidence spectrum.

[b]Not placed in decay scheme.

[c]Weak member of singles multiplet enhanced in coincidence spectrum.

Table 4. (Continued)

Transition Number	Energy (keV)	Relative Intensity
19	555.30 ± 0.5[c]	
20	562.80 ± 0.1	40 ± 4
21	637.81 ± 0.5[c]	
22	661.01 ± 0.3	3.7 ± 0.4
23	768.81 ± 0.5	2.7 ± 0.4
24	774.44 ± 0.5	2.8 ± 0.4
25	804.31 ± 0.3	1.7 ± 0.3
26	902.19 ± 0.3[b]	4.1 ± 0.6
27	905.11 ± 0.3	2.0 ± 0.3
28	937.65 ± 0.3	2.6 ± 0.5

spectra. An intensity was assigned to the 172 keV peak by requiring SKLN to fit a component at that energy to the ~ 174 keV peak in the singles spectrum. Peak parameters (FWHM and skewness) were taken to be the same as for the 182 keV peak of ^{226}Ra in the calibration run. A comparison of the SKLN fits with and without a 172 keV peak is shown in Figure 27. The slight improvement of the 174 keV peak by the inclusion of this component is not sufficient evidence for its existence. However, the 174 keV coincidence spectrum shows the 172 keV transition (Figure 30) in coincidence with the 174 keV gamma ray and justifies including it in the decay scheme.

2. Coincidence data

The ungated spectrum from the coincidence detector is shown in Figure 28, and the resulting coincident spectra are shown in Figures 29, 30, 31, and 32. The background spectrum for the 136, 174, and 210 keV gamma rays is shown in Figure 33. No gamma rays were seen in coincidence with the 563 keV gamma ray and this spectrum is not shown.

The statistics in these coincidence experiments are poor. This is due partially to the low intensity, short-lived sources, and partially to the nature of the Ge(Li)-Ge(Li) coincidence experiment. However, because of the clean spectrum and sharp peaks which result, coincident gamma rays can easily be identified by comparison with the ungated spectrum (Figure 28).

The results of the Ge(Li)-Ge(Li) coincidence measurements shown in Figures 29-32 are summarized in Table 5.

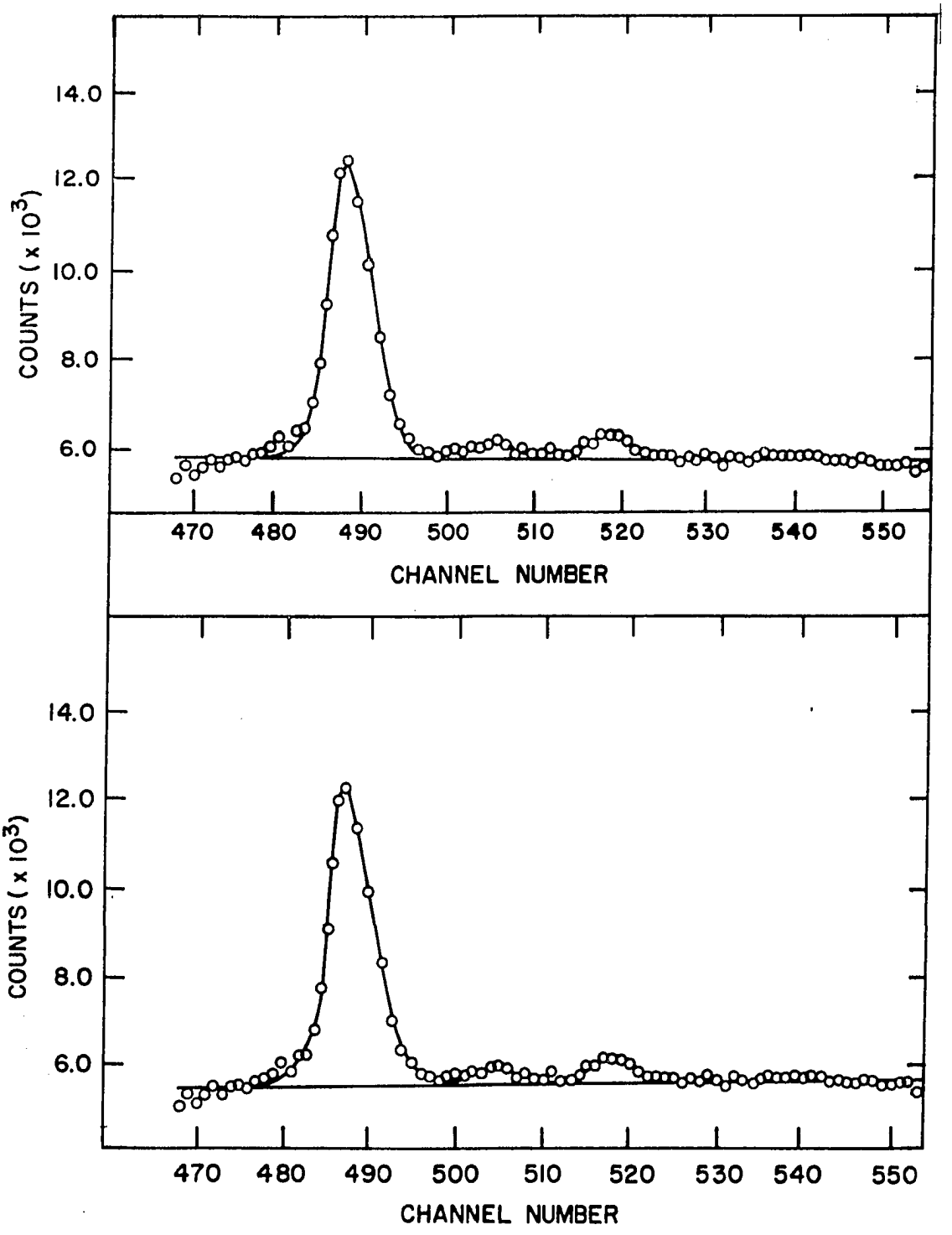

Figure 27. Computer fits without 172 keV component (top) and with 172 keV component (bottom)

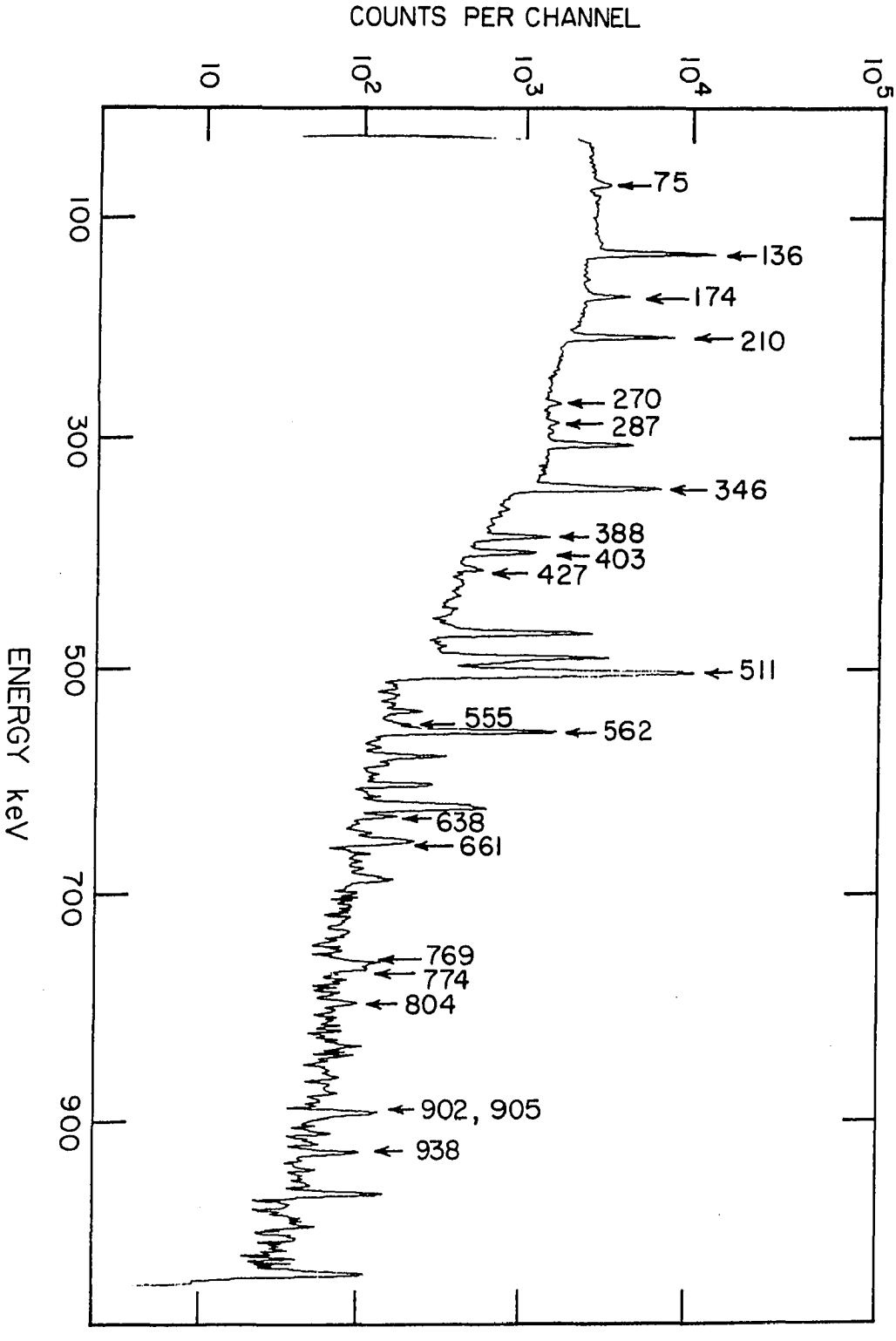

Figure 28. The ungated spectrum from the coincidence detector

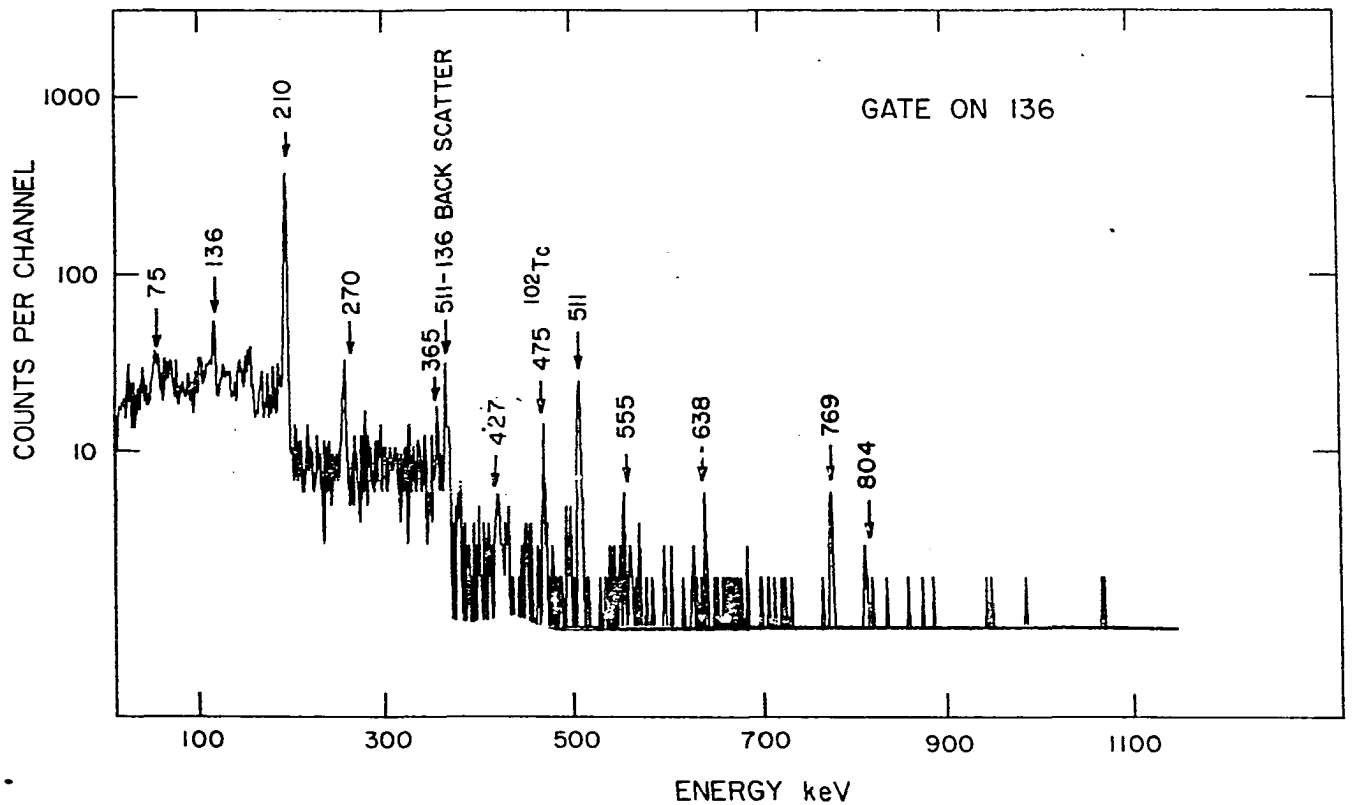

Figure 29. Ge(Li)-Ge(Li) coincidence spectrum of ^{103}Tc gamma rays gated by the 136 keV gamma ray

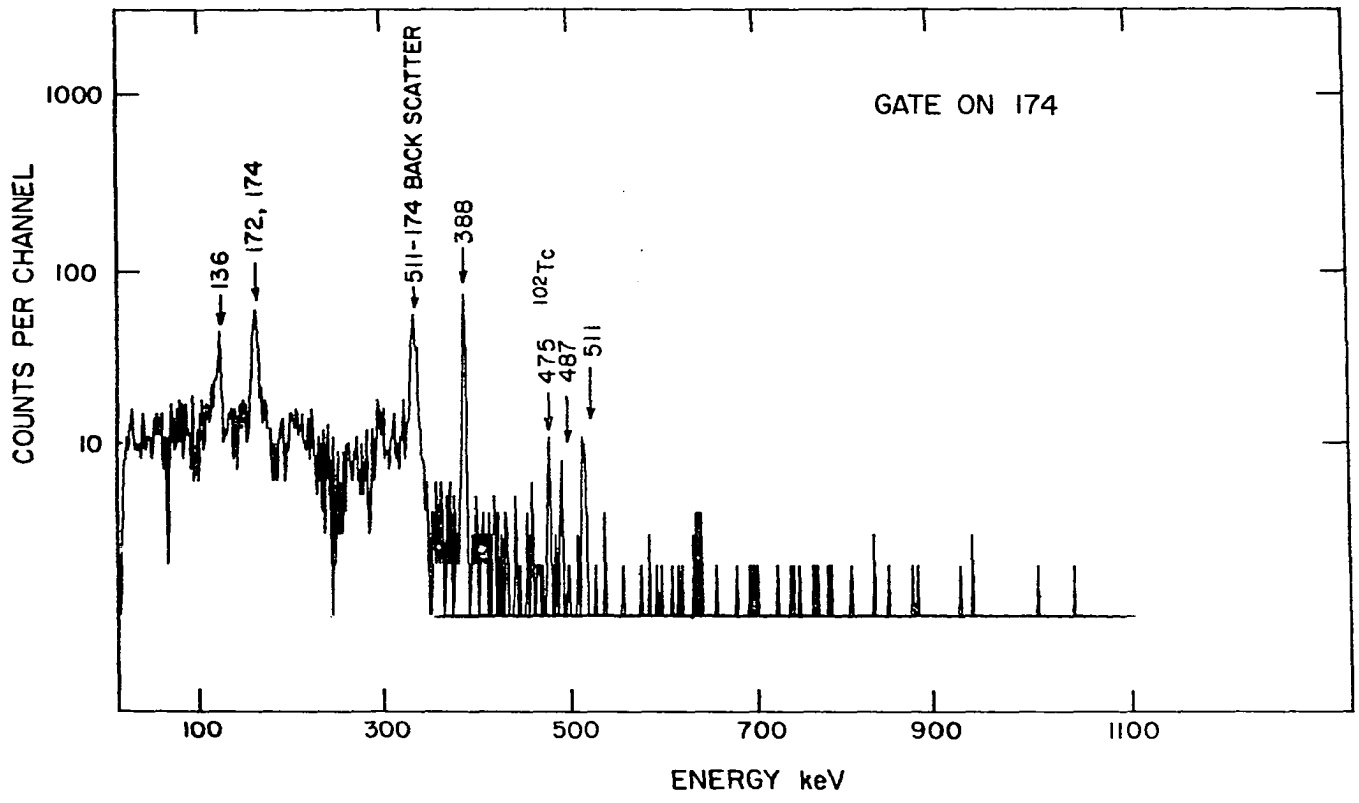

Figure 30. Ge(Li)-Ge(Li) coincidence spectrum of ^{103}Tc gamma rays gated by the 174 keV gamma ray

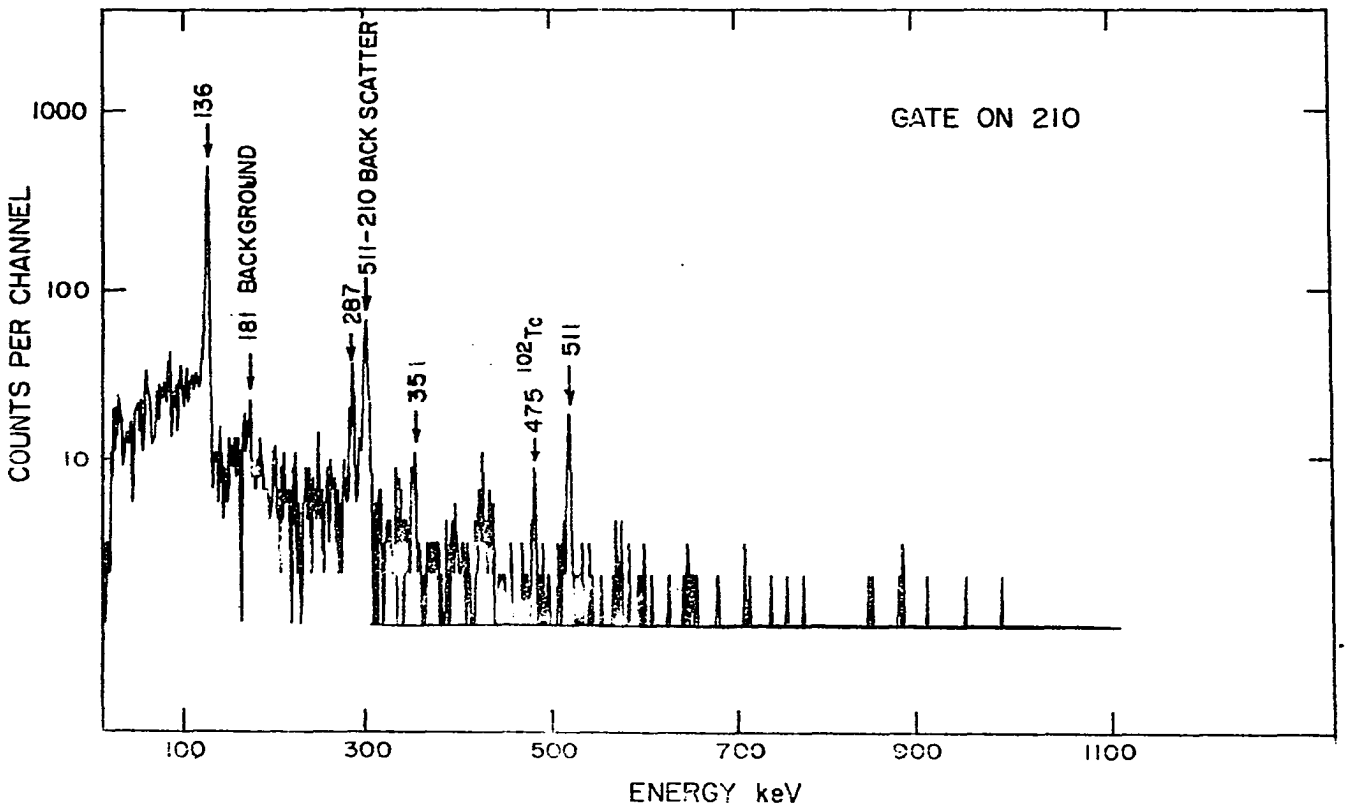

Figure 31. Ge(Li)-Ge(Li) coincidence spectrum of ^{103}Tc gamma rays gated by the 210 keV gamma ray

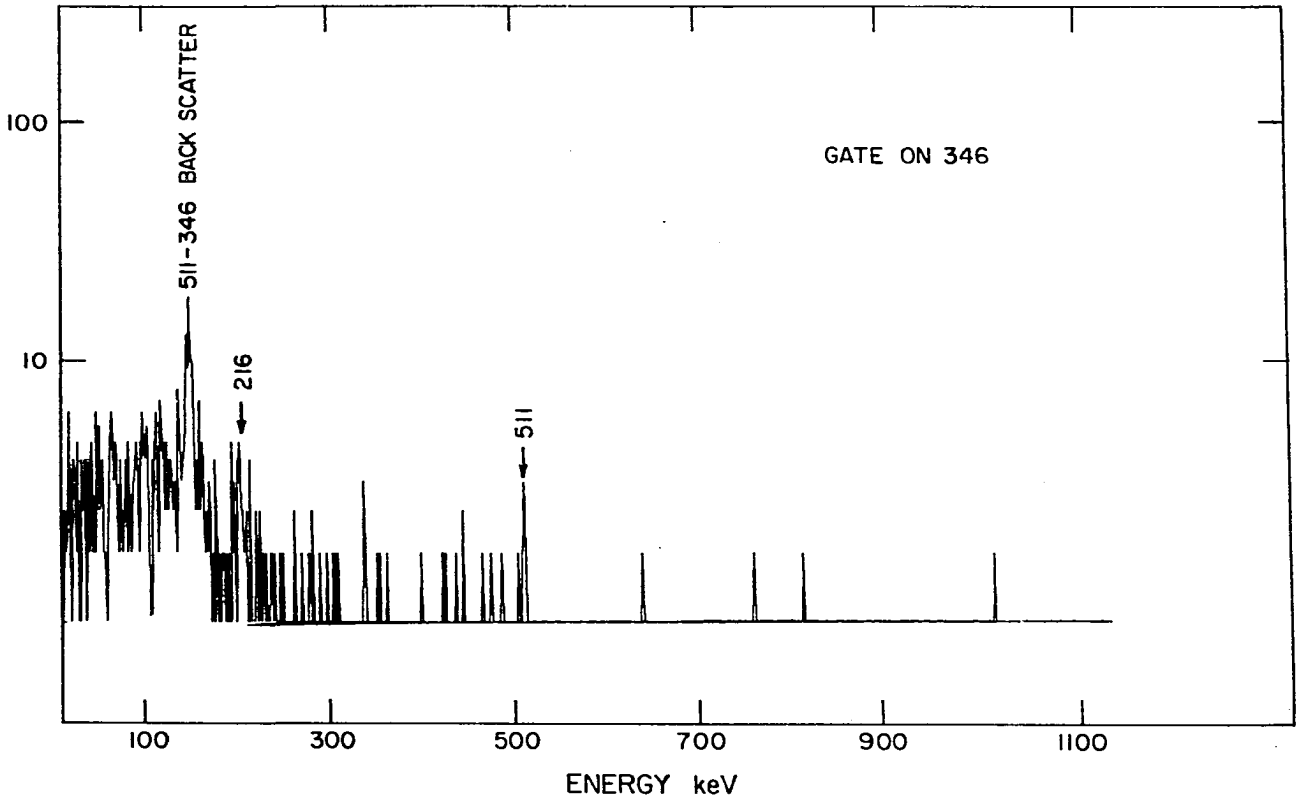

Figure 32. Ge(Li)-Ge(Li) coincidence spectrum of ^{103}Tc gamma rays gated by the 346 keV peak

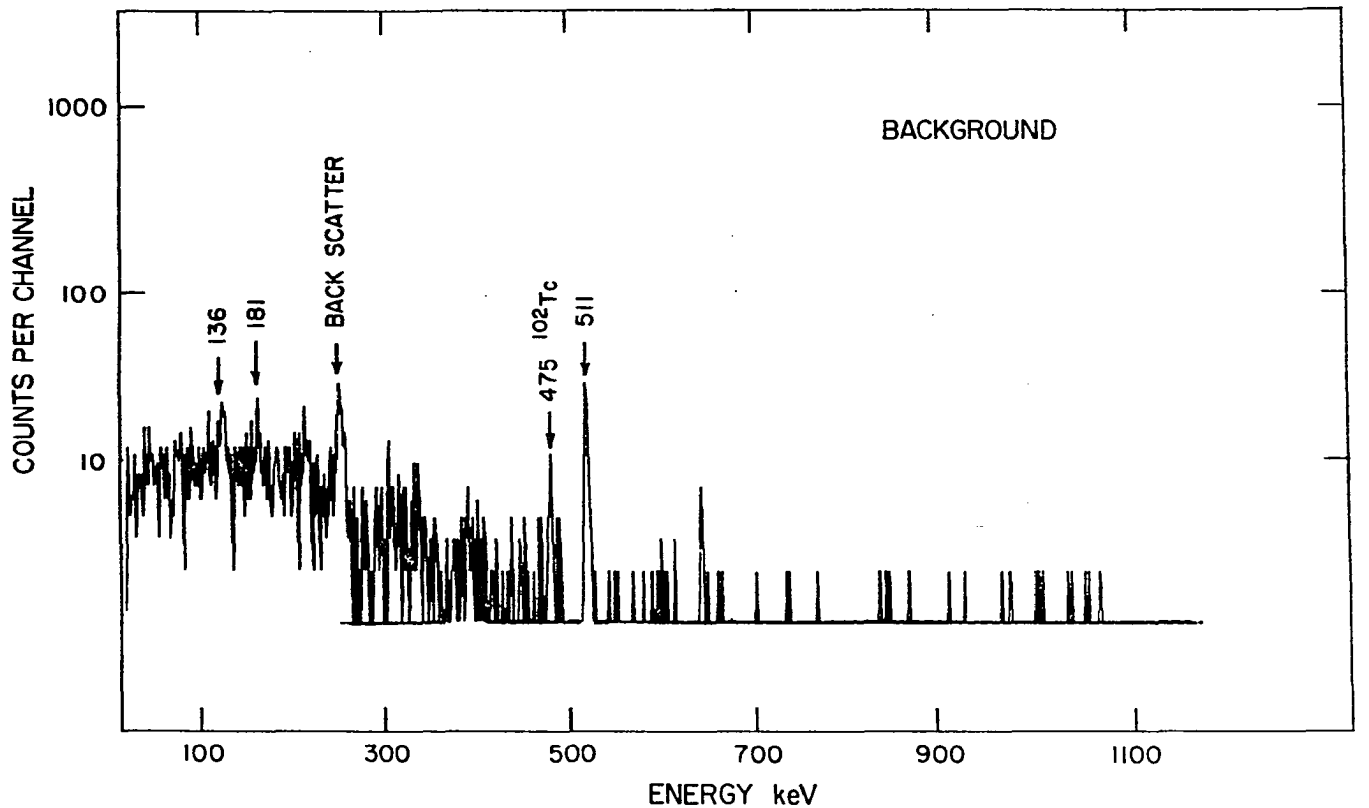

Figure 33. Background spectrum for the 136, 174, and 210 keV gamma rays

Table 5. Coincidences observed in the decay of ^{103}Tc

Energy of gating gamma ray (keV)	Coincident gamma-ray energy (keV)
136.0	136[a], 210, 270, 365, 427, 555, 638, 769, 804
174.2	136[a], 172, 388, 487
210.3	136, 287, 351
346.2	216
562.8	None

[a]See explanation in text.

3. Decay scheme

The decay scheme for ^{103}Tc was constructed using the energy, intensity, and Ge(Li)-Ge(Li) coincidence results of this experiment and the reaction data reported by Diehl et al. (34). The most intense transition at 136 keV was placed as a ground state transition from the 136 keV level in agreement with the level at 133 keV reported by Diehl et al.

The 346 keV gamma ray is the next most intense gamma ray in the spectrum and is also placed as a ground state transition from the level at 346 keV. This level agrees with the level at 343 keV reported by Diehl et al. The transition at 210 keV can be placed as de-exciting the level at 346 keV through the 210-136 keV cascade or it can be placed as a ground state transition from the 210 keV level reported by Diehl et al. The existence of a level at 210 keV allows the placement of the

136 keV gamma ray as de-exciting the 346 keV level through a 136-210 keV cascade, in addition to its placement as a ground state transition. However, the 136 keV transition is almost twice as intense as the 210 keV transition in the singles spectrum (Figure 21). Since there are no other intense gamma rays in coincidence with either the 136 or 210 keV transition, it is not possible to estimate how much of the intensity of the 136 and 210 keV gamma rays is due to ground state transitions from these respective levels. It is certain that the 136 keV and 210 keV ground state transitions are occurring from the other transitions which appear in their respective coincidence spectra.

The remaining intense transition at 563 keV is also placed as a ground state transition. A 563 keV level was not reported by Diehl et al., but no gamma rays were seen in the 563 keV coincidence spectrum which indicates it is probably a ground state transition. This is verified further by the 216-346, 210-351, and 136-427 keV coincidences.

The levels at 406, 497, 661, 691, and 905 keV are verified by the coincidence data of this experiment. They correspond to the levels at 402, 497, 658, 693, and 902 keV seen in the (d,t) work of Diehl et al.. In addition to the level at 563, levels at 501, 774, and 940 keV are established by the coincidence data and are not seen in the reaction experiments.

To account for the gamma rays with energy 343, 403, and 938 keV, a level at 2.7 keV is postulated. The energy sums for these gamma rays feeding this level agree within experimental error to energies of known levels.

The decay scheme which results from the above arguments is shown in Figure 34. The reaction experiments of Diehl et al. (34) and Nolen et al. (35) are included as indicated by the key. Asterisks denote the two possible placements of the 136 and 210 keV transitions.

4. Discussion

The decay scheme shown in Figure 34 includes 24 gamma rays which had not been previously assigned to the decay of ^{103}Tc by Kienle et al. (31). The levels which could be populated by beta decay and which are identified in this experiment agree very well with the (d,t) reaction work of Diehl et al. (34). All the positive parity levels with $3/2 \leq J \leq 7/2$ reported by Diehl et al. are seen in this experiment. The $7/2^+$ level at 240 keV reported by Nolen et al. (35) is not seen in this experiment or in the work of Diehl et al. This is not unreasonable since the ^{102}Ru(d,p)^{103}Ru experiment would be expected to excite different states than the ^{104}Ru(d,t)^{103}Ru reaction. The (d,t) reaction and this experiment should see the same levels since both experiments are related to a neutron hole in the product nucleus.

The apparent beta feeding of levels with spins 5/2 and 7/2 implies that the ground state of ^{103}Tc should be a $5/2^+$ or a $7/2^+$ level, in contrast to the $9/2^+$ quantum numbers for the ground state of $^{95, 97, 99, 101}$Tc. The level at 406 keV has a net 15% relative intensity imbalance in the gamma rays into and out of this level. If this level is $3/2^+$ as tentatively assigned by Diehl et al., this would eliminate the possibility of $J^\pi = 7/2^+$ or $9/2^+$ for the parent nucleus. The level at 136 keV also has a tentative spin and parity of $3/2^+$, but the existence of two

Figure 34. Decay scheme for ^{103}Tc. The numbering of the transitions corresponds to their order in Table 4. The coincidence results are shown by dots, at the start of an arrow to label a gating transition and at the tip to indicate an enhanced line

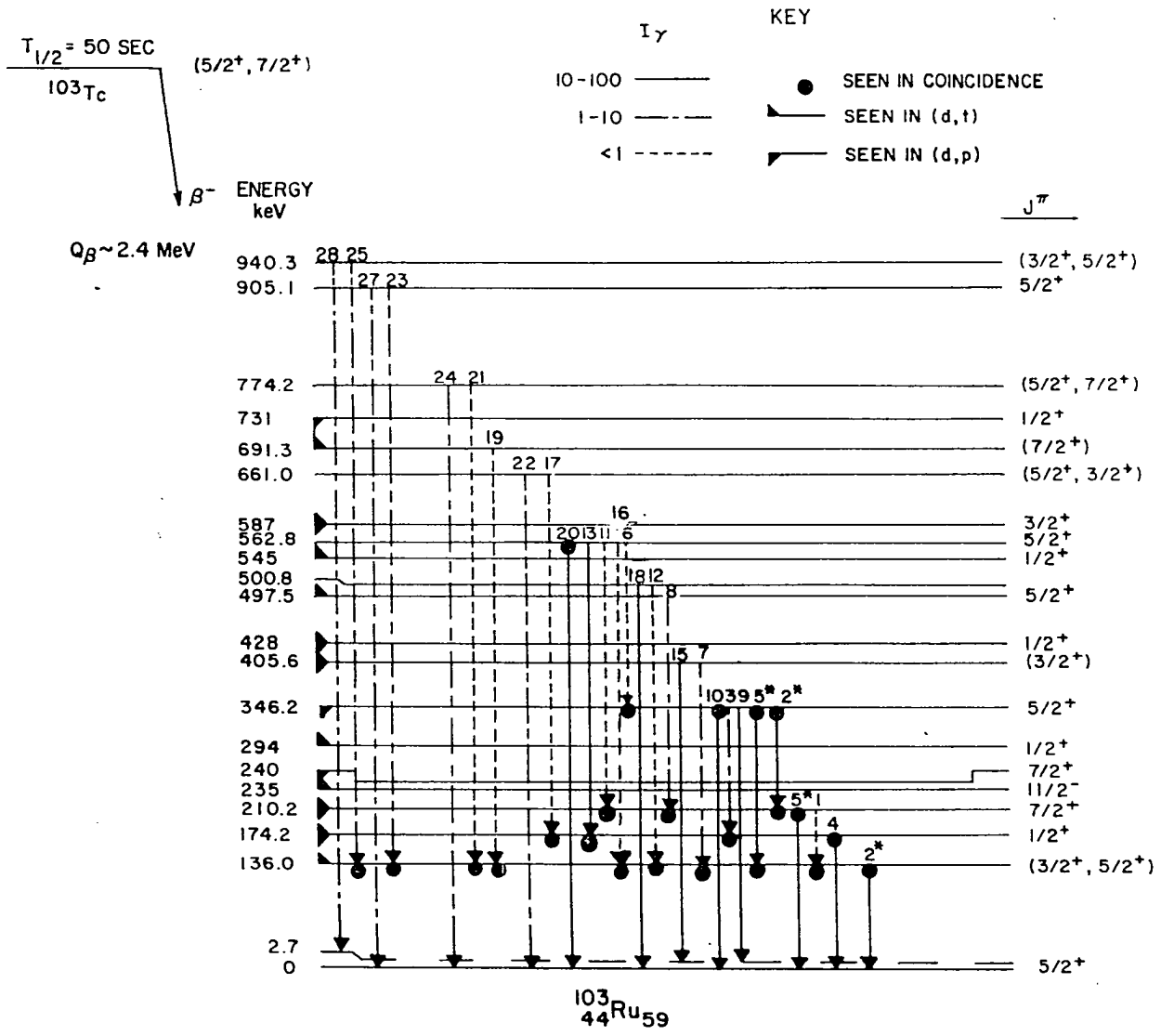
$T_{1/2}$ = 50 SEC
^{103}Tc
$(5/2^+, 7/2^+)$
β^-
$Q_\beta \sim 2.4$ MeV
I_γ
KEY
10-100
1-10
<1
SEEN IN COINCIDENCE
SEEN IN (d,t)
SEEN IN (d,p)
ENERGY keV
J^π
940.3
905.1
774.2
731
691.3
661.0
587
562.8
545
500.8
497.5
428
405.6
346.2
294
240
235
210.2
174.2
136.0
2.7
0
$(3/2^+, 5/2^+)$
$5/2^+$
$(5/2^+, 7/2^+)$
$1/2^+$
$(7/2^+)$
$(5/2^+, 3/2^+)$
$3/2^+$
$5/2^+$
$1/2^+$
$5/2^+$
$1/2^+$
$(3/2^+)$
$5/2^+$
$1/2^+$
$7/2^+$
$11/2^-$
$7/2^+$
$1/2^+$
$(3/2^+, 5/2^+)$
$5/2^+$
$^{103}_{44}Ru_{59}$

possible placements of the 136 keV gamma ray does not allow the calculation of the intensity imbalance out of the 136 keV level.

It appears that there is a weak 136 keV transition in both the 136 and 174 keV gated spectra which cannot be accounted for entirely by the background (Figures 29, 30, and 33). Since a 75 keV gamma ray appears in coincidence with the 136 keV transition, some of the 136-75-136 keV cascade could be expected. It is also possible that there is a 38 keV transition from the 174 to the 136 keV level which would allow a 172-38-136 keV cascade to take place, since a gate on the 174 keV transition would also gate on the 172 keV gamma ray of this closely spaced doublet. However, the appearance of this weak 136 keV coincidence can also be explained as incomplete background subtraction, as was done in Section II., D.. The background window is again set on a lower portion of the Compton background than either the 136 or 174 keV peaks (Figure 23). In either case the experimental results are not affected.

It was mentioned earlier that a gamma ray of energy $\sim$ 210 keV and half-life 1.7 milliseconds (32, 33) is identified with an isomeric state in ^{103}Ru. Since Diehl et al. (34) have identified a $11/2^-$ level at 235 keV, a possible explanation is that the 235 keV level decays via an M2 transition to the 210 keV (spin and parity $7/2^+$) which decays promptly to the ground state. The Weisskopf estimate of the half-life for a 20 keV M2 transition is approximately 10^{-3} seconds (28). This good agreement with experiment can be expected, since the $11/2^-$ level should be a rather pure single particle state (Figure 1).

IV. CONCLUSIONS

A. Decay of ^{95}Ru

The energy level structure of ^{95}Tc deduced from this experiment is similar to that of neighboring odd-A even-N nuclei (28). A comparison with two of the other technetium isotopes is shown in Figure 35 (20, 50). The $1/2^-$ isomeric state is common in these nuclides corresponding to the $(1g_{9/2})^n(2p_{1/2})^1$ (n even) configurations with the $g_{9/2}$ protons coupled to zero spin. A pair of negative parity states with J = 3/2 and 5/2 usually are found at about 1 MeV excitation, corresponding to the $g_{9/2}$ protons being coupled to J = 2. The 927 keV level in ^{95}Ru is tentatively identified as $5/2^-$, but the $3/2^-$ state has not been found. On the basis of its decay to the $1/2^-$ level, the state at 1049 keV could be the missing $3/2^-$ state, since the uncertainty in the log(ft) value could make it consistent with first forbidden beta decay (spin change of 1 and change of parity).

A large number of positive parity levels also occur in these nuclei, corresponding to $(2p_{1/2})^2(1g_{9/2})^m$ or $(2p_{1/2})^0(1g_{9/2})^{m+2}$ proton configurations (m odd). The positive parity level sequence $9/2^+$, $7/2^+$, $5/2^+$ is common, with the spacing decreasing as Z or N increases. The number of positive parity states which can occur for an arbitrary number of protons in the $g_{9/2}$ orbital is related to the seniority quantum number. The $g_{9/2}$ orbital is of particular theoretical interest since J = 9/2 is the lowest J value for which the seniority might not be a good quantum number (6). One of the nice features of the effective interaction

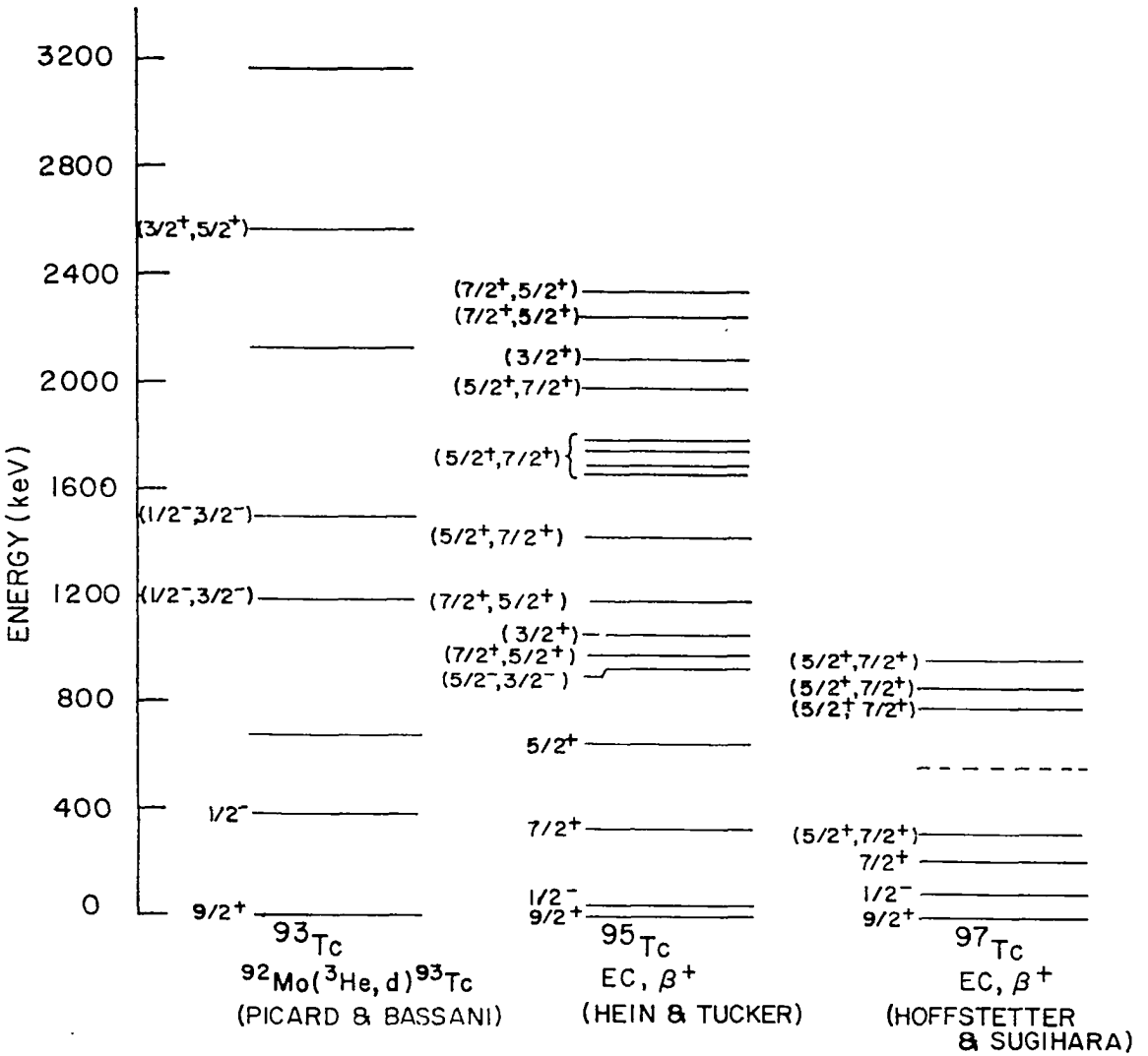

Figure 35. Comparison of experimental levels of three odd-A technetium isotopes

calculations mentioned in Section I., A. is that the positive parity levels are almost pure seniority configurations (6).

The effective interaction calculations of Vervier (11) using ^{88}Sr as the inert core and Bhatt and Ball (9) using ^{90}Zr as the inert core are compared with the results of this experiment in Figure 36. Both calculations did not include the negative parity states, but these could easily be included and their absence should not be considered in an evaluation of the theory. The low spin sequence ($J < 9/2$) for the first few excited states is consistent with this experiment, but the energy spacings are too large. Since agreement between these theories and experimental results are better for N = 50 nuclei, for example ^{93}Tc (45, 46, 20) and ^{91}Nb (51), the neutrons may have a more complex configuration than $(2d_{5/2})^2$. Another possibility is that the positive parity states are not as pure seniority configurations as thought by Talmi and Unna (6).

A future study of the levels of ^{95}Tc might include $^{96}Ru(d, ^3He)$, $^{96}Ru(t,\alpha)$, and $^{94}Mo(^3He, d)$ reaction studies which could assign definite spins and parities to levels already known. The $^{93}Nb(\alpha, 2n\ \gamma)$ reaction could excite the higher spin states which are not seen in the radioactive decay work due to the beta decay selection rules. Future theoretical work might consider the contribution of the extra neutrons and the possibility of mixed seniority configurations.

B. Decay of ^{103}Tc

The elementary single particle shell model predicts $J^\pi = 7/2^+$ for the ground state of ^{103}Ru corresponding to a $(2d_{5/2})^6(1g_{7/2})^3$

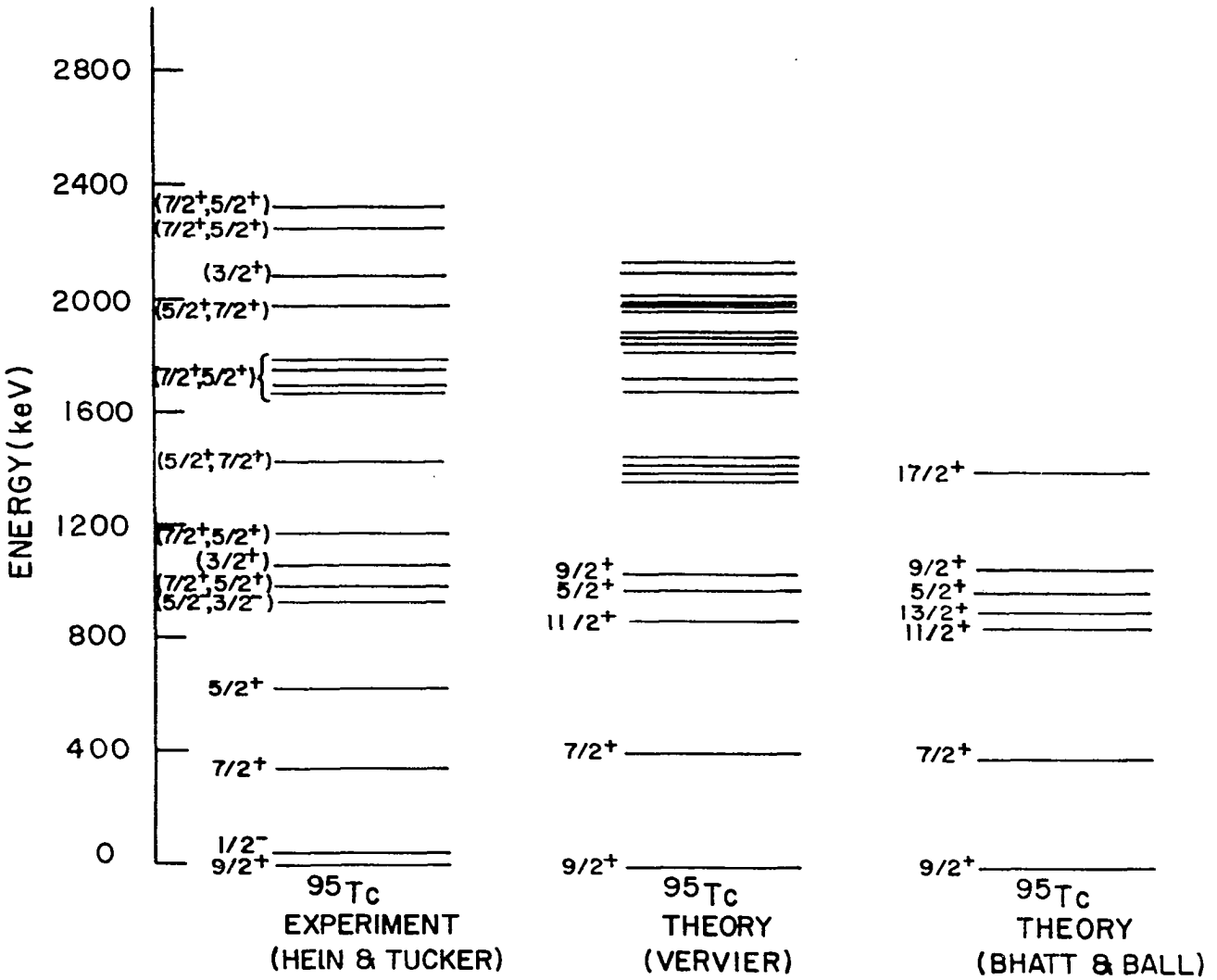

Figure 36. Comparison of experimental results with theoretical calculations for levels in ^{95}Tc

configuration of the neutrons outside the closed N = 50 core. However, the experimental value of $5/2^+$ corresponding to a neutron hole in the $2d_{5/2}$ orbital indicates the configuration is probably $(1g_{7/2})^4(2d_{5/2})^5$. This can be accounted for by including pairing effects in the elementary model. Most of the levels are probably an admixture of several configurations of the type $(1g_{7/2})^m(2d_{5/2})^n$ $(n + m = 9)$ and the problem is hard to treat in the simple shell model picture. The low lying $11/2^-$ level (Figure 33) is characteristic of the odd neutron nuclei in this region (34) and corresponds to a single particle excitation into the $1h_{11/2}$ orbital (Figure 1) of the odd neutron.

The ground state spin and parity of ^{103}Tc is probably $5/2^+$ or $7/2^+$ from the spin and parity of the levels fed in beta decay. The apparent feeding of the tentative $3/2^+$ levels seems to favor the $5/2^+$ assignment. For comparison, ^{105}Rh is thought to have spin and parity $7/2^+$ (4, 28), while ^{107}Rh is thought to have spin and parity $5/2^+$ (4, 28). It may be that the ^{103}Tc ground state is either the $7/2^+$ or $5/2^+$ of the $(2p_{1/2})^2(1g_{9/2})^3$, $(1g_{9/2})^5$ configurations characteristic of nuclei in this region. These levels seem to approach 0 keV excitation as the number of neutrons is increased (28). In the deformed model, a deformation, ϵ, between -0.1 and -0.2 can give either a $7/2^+$ or a $5/2^+$ (28) corresponding to the 7/2 [413] or 5/2 [422] Nilsson states. In any case, the ^{103}Tc ground state is not a $9/2^+$ as the other technetium isotopes are (28).

Future studies on the decay of ^{103}Tc should remeasure the beta spectrum to see if beta feeding to the ^{103}Ru ground and 210 keV states

can be seen. The short half-life makes beta-ray spectroscopic measurements difficult. From these decay studies, it might be possible to determine the intensity of the ground state transitions from the 210 and 136 keV levels.

In addition, a ^{104}Ru(d, p) reaction experiment could fix the spin and parity of the ^{103}Tc ground state. It would also give information about other levels in ^{103}Tc which could be used for theoretical comparisons in this mass region.

V. LITERATURE CITED

1. Haxel, O., Jensen, J. H. D., and Suess, H. E., Modellmäβige deutung der ausgezeichneten nukleonenzahlen in kernbau, Z. Physik 128, 295 (1950).

2. Mayer, M. G., Nuclear configurations in the spin-orbit coupling model. I. Empirical evidence, Phys. Rev. 78, 16 (1950).

3. Mayer, M. G. and Jensen, J. H. D., Elementary theory of nuclear shell structure (John Wiley and Sons, Inc., New York, N.Y., 1955).

4. Goldman, D. T. and Stehn, J. R., Chart of the nuclides, (General Electric Co., New York, N.Y., 1968).

5. Bayman, B. F., Reiner, A. S., and Sheline, R. K., Levels in Zr^{90}: theoretical, Phys. Rev. 115, 1627 (1959).

6. Talmi, I. and Unna, I., Energy levels and configuration interactions in Zr^{90} and related nuclei, Nucl. Phys. 19, 225 (1960).

7. Kisslinger, L. S. and Sorensen, R. A., Spherical nuclei with simple residual forces, Rev. Mod. Phys. 35, 853 (1963).

8. Cohen, S., Macfarlane, M. H., and Soga, M., The effective interaction and identical-nucleon seniority for nuclei near Zr^{90}, Phys. Letters 10, 195 (1964).

9. Bhatt, K. H. and Ball, J. B., Nuclear spectroscopy of the isotopes of Nb, Mo, and Tc, Nucl. Phys. 63, 286 (1965).

10. Auerbach, N. and Talmi, I., Energy levels, configuration mixing and proton neutron interaction in the Zr region, Nucl. Phys. 64, 458 (1965).

11. Vervier, J., Effective nucleon-nucleon interactions in the Y, Zr, Nb, Mo and Tc isotopes, Nucl. Phys. 75, 17 (1966).

12. Stautberg, M. M., Kraushaar, J. J., and Ridley, B. W., Nuclear structure studies of Sr^{88} and Y^{89} using 19-Mev proton scattering and the $^{88}Sr(He^3,d)$ reaction, Phys. Rev. 157, 977 (1967).

13. Kavaloski, C. D., Lilly, J. S., Shreve, D. C., and Stein, N., (d,He^3) studies on Zr^{90}, Y^{89}, and Sr^{88}, Phys. Rev. 161, 1107 (1967).

14. Cosman, E. R. and Slater, D. C., Nuclear-reaction studies in the strontium isotopes: neutron particle hole states in Sr^{88} and the $Sr^{87}(d,p)Sr^{88}$ reaction, Phys. Rev. 172, 1126 (1968).

15. Glover, R. N. and McGregor, A., Shell effects in the excitation of 0^+ states by (t.p) reactions, Phys. Letters 24B, 97 (1967).

16. Pettersson, H., Antman, S., and Gunditz, Y., The decay of ^{90}Nb, Nucl. Phys. A108, 124 (1968).

17. Dickens, J. K., Eichler, E., and Satchler, G. R., $^{90, 92, 94}Zr(p, p')$ reactions at 12.7 MeV, Phys. Rev. 168, 1355 (1968).

18. Ball, J. B. and Fulmer, C. B., Neutron hole states in Z = 40 nuclei studied with the (p,d) reaction on ^{90}Zr, ^{91}Zr, and ^{92}Zr, Phys. Rev. 172, 1199 (1968).

19. Vourvopoulos, G. and Fox, J. D., Experimental study of the $T=T_z$ state in ^{90}Zr via a $(^3He,d)$ reaction, Phys. Rev. 177, 1558 (1968).

20. Picard, J. and Bassani, G., Spectroscopic studies in the A=90 mass region, Nucl. Phys. A131, 636 (1969).

21. Cates, M. R., Nuclear structure studies in the mass-90 region with the $(^3He,d)$ reaction. Unpublished Ph.D. thesis. College Station, Texas, Library, Texas A & M University. 1969.

22. Preston, M. A., Physics of the nucleus (Addison-Wesley Publishing Company, Inc., Reading, Massachusetts, 1962).

23. Eggen, D. T. and Pool, M. L., Radioactive isotopes of Ru and Tc, Phys. Rev. 74, 57 (1948).

24. Riehs, P. and Warhanek, H., Das zerfallschema von Ru^{95}, Nucl. Phys. A125, 164 (1963).

25. Heuer, D., Der zerfall des ruthenium 95, Z. Physik 201, 142 (1967).

26. Pinston, J. A., Monnand, E., and Moussa, A., Désintégration de ^{95}Ru, J. Physique 29, 257 (1968).

27. Kim, H. J., Robinson, R. L., Johnson, C. H., and Raman, S., Energy levels of ^{91}Nb, ^{93}Mo, ^{95}Tc and ^{92}Tc via (p,n) reactions and the reaction Q-values, Nucl. Phys. A142, 35 (1970).

28. Lederer, C. M., Hollander, J. M., and Perlman, I., Table of isotopes, 6th ed. (John Wiley and Sons, Inc., New York, N.Y., c1967).

29. Hager, R. S. and Seltzer, E. C., Internal conversion tables. Part I: K-, L-, M-shell conversion coefficients for Z = 30 to Z=103, Nuclear Data A4, 1 (1968).

30. Ball, J. B., A study of the levels in ^{95}Ru with the ^{96}Ru(p,d) reaction, (Abstract) Bull. Am. Phys. Soc. 15, 551 (1970).

31. Kienle, P., Wien, K., Zahn, U., and Weckermann, B., Die β-zerfallsenergie der technetiumisotope Tc^{103}, Tc^{104} und Tc^{105}, Z. Physik 176, 226 (1963).

32. Brandi, K., Engelmann, R., Hepp, V., Kluge, E., Krehbiel, H., and Meyer-Berkhaut, U., Investigations of short-lived isomeric states with half-lives in the μs and ms region, Nucl. Phys. 59, 33 (1964).

33. Gabsdil, W., The isomers ^{101m}Tc, ^{103m}Ru, ^{155m}Tb, ^{208m}Bi, Nucl. Phys. A120, 556 (1968).

34. Diehl, R. C., Cohen, B. L., Moyer, R. A., and Goldman, L. H., Nuclear-structure studies with (d,t) reactions on Pd^{110}, Pd^{108}, and Ru^{104}, Phys. Rev. C 1, 2086 (1970).

35. Nolen, J. A., Fortune, H. T., Kienle, P., and Morrison, G. C., Energy levels of ^{103}Ru and ^{105}Ru from the $^{102, 104}$Ru(d,p) reactions, Argonne National Laboratory Report ANL-7481 (Argonne National Laboratory, Argonne, Illinois, 1968).

36. Unik, J. P. and Rasmussen, J. O., Decay schemes of the isomers Tc^{95} and Tc^{97}, Phys. Rev. 195, 1687 (1959).

37. Hammer, C. L. and Bureau, A. J., Method for the prompt destruction of the electron beam in a synchrotron. I, Rev. Sci. Instr. 26, 594 (1955).

38. Hammer, C. L. and Bureau, A. J., Method for the prompt destruction of the electron beam in a synchrotron. II, Rev. Sci. Instr. 26, 598 (1955).

39. Bureau, A. and Hammer, C., Procedure for making intense sources in an electron synchrotron, Rev. Sci. Instr. 32, 93 (1961).

40. Orphan, V. J. and Rasmussen, N. C., A pair spectrometer using a large coaxial lithium-drifted germanium detector, I.E.E.E. Trans. Nucl. Sci. NS-14, 544 (1967).

41. Simmons, S. O., Construction of a three crystal spectrometer and a study of the decay of ^{90}Nb. Unpublished Ph.D. thesis. Ames, Iowa, Library, Iowa State University of Science and Technology. 1970.

42. Ewan, G. T. and Travendale, A. J., High-resolution studies of gamma-ray spectra using lithium-drift germanium gamma-ray spectrometers, Can. J. Phys. 42, 2286 (1964).

43. Larsen, J. T., Gamma ray decay schemes for ^{142}Xe, ^{142}Cs, ^{142}Ba, ^{142}La. Unpublished Ph.D. thesis. Ames, Iowa, Library, Iowa State University of Science and Technology. 1970.

44. Gunnick, R., Niday, J. B., Anderson, R. P., and Meyer, R. A., Gamma-ray energies and intensities, Lawrence Radiation Laboratory Report UCID-15439 (Lawrence Radiation Laboratory, Livermore, California, 1969).

45. Reitmann, D. and Engelbrecht, C. A., Scattering of fast neutrons from natural Zr and Nb, Nucl. Phys. 48, 593 (1963).

46. Engelbrecht, C. A., The excited states of Nb^{93}, Phys. Letters 4, 213 (1963).

47. Rogers, V. C., Beghian, L. E., Clikeman, F. M., Hofman, F., and Wilensky, S., Nuclear structure studies of ^{93}Nb using the ^{93}Nb(n, n'γ) and ^{93}Nb(p,p'γ) reactions, Nucl. Phys. A142, 100 (1970).

48. Cook, W. B., The decay of 67 hour ^{99}Mo, Nucl. Phys. A139, 277 (1969).

49. Jones, A. D. W., Becker, R. E., McDonald, R. E., and Poletti, A. R., Beta decay of Na^{25} and Al^{29}, Phys. Rev. C 1, 1000 (1970).

50. Hofstetter, K. J. and Sugihara, T. T., Decay of ^{97}Ru, ^{97}Zr, ^{97}Nb, Nucl. Phys. A140, 658 (1970).

51. Hesse, K. and Finckh, E., The decay of ^{91m}Mo and of ^{91g}Mo, Nucl. Phys. A141, 417 (1970).

VI. ACKNOWLEDGMENTS

I wish to express my sincere gratitude to Dr. A. B. Tucker for his valuable assistance throughout the course of these investigations. I am also grateful to him for the encouragement he has given me in all phases of my graduate career.

I also wish to thank the following people who helped in the course of this research:

Dr. W. L. Talbert, Jr. and the members of Nuclear Physics Group VII for the use of much instrumentation, including 4 germanium detectors.

Dr. R. C. Morrison for the use of a germanium detector.

Dr. J. E. Hall for the use of a germanium detector.

Dr. J. T. Larsen for assistance with the computer programs used in the analysis of the data.

Dr. A. J. Bureau, Mr. G. Holland, and Mr. J. Sayre for their assistance in the production of the radioactive sources.

Mr. K. Malaby for the use of the counting lab and for the making of the calibration sources.

The Department of Health, Education, and Welfare for the financial support given me during my graduate work.